Science of the Total Environment 957 (2024) 177479

Contents lists available at ScienceDirect

Science of the Total Environment

journal homepage: www.elsevier.com/locate/scitotenv

Morphodynamics drive the transport and accumulation of anthropogenic microparticles in tropical coastal depositional systems in southeastern Brazil

Isabela Furlan [a,*], Milene Fornari [a,*], André Oliveira Sawakuchi [b], Paulo César Fonseca Giannini [b], Jessica Dipold [c], Anderson Zanardi de Freitas [c], Niklaus Ursus Wetter [c], Décio Semensatto [d]

[a] Biosciences Institute, São Paulo State University (UNESP), São Vicente 11330-900, Brazil
[b] Institute of Geosciences, University of São Paulo (USP), São Paulo 05508-080, Brazil
[c] Nuclear and Energy Research Institute (IPEN), University of São Paulo (USP), São Paulo 05508-000, Brazil
[d] Department of Environmental Sciences, Federal University of São Paulo (UNIFESP), Diadema 09972270, Brazil

HIGHLIGHTS

- Detailed characteristics of anthropogenic microparticles (AMP) are investigated in different coastal features and waters.
- Fiber are AMP dominant: >95 % in sediments, 95 % estuarine water and 80 % marine water.
- Transport and deposition of AMP primarily respond to hydro-wind dynamic sorting processes.
- Sediments are the main sink, and water is the primary source of AMP in the coastal environment.

GRAPHICAL ABSTRACT

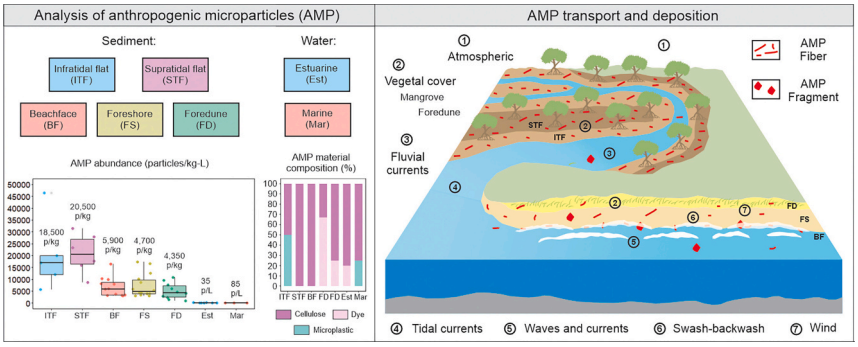

ARTICLE INFO

Editor: Julian Blasco

ABSTRACT

A significant limitation in current coastal pollution research is that microplastics (<5 mm) comprise only a fraction of all anthropogenic microparticles (AMP, <5 mm) scale residues. Comprehensive AMP assessments, including those comprising semisynthetic, and modified natural compositions, are lacking. For instance, the accumulation of AMP in different coastal morphological features within a depositional system remains poorly known, fueling long-lasting debates about the distribution process of microparticles. Using a multi-proxy approach, we address mutual interactions between distinct surface morphologies (tidal flats, beaches, and foredunes) and transport and deposition dynamics of AMP. This issue was addressed by analyzing sediment and water samples collected at a marine protected area in the south coastal of São Paulo (Brazil). Here, we showed that AMP abundance in the tidal mudflat (18,500–20,500 particles/kg) was four times higher than in beach sands (4700–5900 particles/kg), while the lowest abundance was observed in foredune sands (4350 particles/kg). This can be attributed to the low-energy hydrodynamics of tidal flats associated with the cohesive behavior of muddy

* Corresponding authors.
E-mail addresses: isabela.furlan@unesp.br (I. Furlan), milene.fornari@unesp.br (M. Fornari).

https://doi.org/10.1016/j.scitotenv.2024.177479
Received 8 December 2023; Received in revised form 5 November 2024; Accepted 8 November 2024
Available online 18 November 2024

sediments, which consequently favor trapping and act as the main sink for AMP. Further, coastal processes (waves and currents) drive AMP onshore through sediment transport from the surfzone to the beach, from where the AMP becomes available for onshore eolian transport. Higher AMP abundance (85 particles/l) was observed in the marine water samples compared to the estuarine water samples (35 particles/l). Fibers <1 mm appeared as the predominant AMP in the sediment (99–100 %) and water (80–95 %) samples, primarily consisting of modified cellulose (73 %), dye signature only (16 %), and microplastics (11 %). Consequently, we argue that to fully comprehend the spatial distribution of AMP in coastal sediments and waters, it is crucial to analyze these microparticles from an integrated perspective, primarily considering the hydro-wind dynamics of different coastal morpho-sedimentary compartments combined with sediment grain size.

1. Introduction

Anthropogenic microparticles (AMP, here used to describe synthetic, semi-synthetic, and dyed particles <5 mm) have become one of the main threats to marine environments (Ostle et al., 2019; Huntington et al., 2020), due to their ubiquitous nature and detrimental effects on the biota and ecosystems (Dehaut et al., 2016). In recent years, synthetic polymers corresponding to microplastics (MP, plastic particles with a size between 1 μm and 5 mm, e.g., Arthur et al., 2009; Hartmann et al., 2019) have been the most widely studied AMP (Aretoulaki et al., 2020). Particular emphasis has been placed on MP of marginal-marine environments, including the surface waters of estuaries (Lima et al., 2014; Xu et al., 2018) and the sea (Zhu et al., 2018; Qi et al., 2020), but also sediments of the mangrove tidal flats (Nor and Obbard, 2014; Zhou et al., 2020), beaches (de Carvalho and Baptista Neto, 2016; Perumal and Muthuramalingam, 2022), and eolian dunes (Liebezeit and Dubaish, 2012; Costello and Ebert, 2020).

However, recent review articles have drawn attention to the fact that synthetic plastic is not the only microparticle (semi-synthetic, modified cellulose) present in marine environments (Barrows et al., 2018; Kim et al., 2021; Athey and Erdle, 2022; Kwak et al., 2022). For example, the majority of microparticles in the world's oceans are dyed cellulose (Suaria et al., 2020). AMP, which include semi-synthetic and modified natural materials, also contain a suite of toxic chemical additives that may cause harmful effects on marine ecosystems (Athey and Erdle, 2022). Notably, this highlights a need for studies with a broader focus on other related microparticles of anthropogenic origins beyond only MPs.

The most common shape of AMP found in coastal ambiences is fibers (e.g., Nor and Obbard, 2014; Fagiano et al., 2023). According to their origin and production process, these can be classified into synthetic fibers (such as MP), semi-synthetic or artificial fibers (such as anthropogenically modified cellulose), and natural fibers (such as cellulose without chemical processing) (Athey and Erdle, 2022). Microfibers can originate from textile materials, personal care products, and cigarette filters (Carr, 2017; Belzagui et al., 2021; and critical review proposed by Athey and Erdle, 2022). For all these particle types, production and release are indisputably associated with anthropogenic activities (e.g., Jorquera et al., 2022), hence their categorization as AMP.

Yet, once the particles reach the marine environment, their spatial and temporal distribution in sediments and water columns can be linked to the hydro-aerodynamics (ocean circulation, winds, tides, waves, and their induced currents), intrinsic characteristics of microparticles (e.g., density, size, shape, and composition), and sedimentary substrate grain size (mud, sand, or mixed) (see Critchell and Lambrechts, 2016; Kane et al., 2020; Waldschläger et al., 2020). The consequences of the storage of microparticles in marine systems are considerable: AMP can be ingested by organisms (Antão-Barboza et al., 2018) and result in bioaccumulation in the food chain (Andrady, 2011), as well as cause adverse effects in these marine organisms due to the absorption of toxic substances (Kwak et al., 2022). Recent studies show that non-plastic AMP have ecotoxicity comparable to synthetic polymers due to chemical additives, dyes, and finishing agents used during their production (Athey and Erdle, 2022).

Given the potential impacts of AMP, including synthetic, semi-synthetic, and modified natural materials, on biota and their wide persistence in natural ambiences, studies that integrate data on their quantification and characterization in sediment and water samples from coastal settings become necessary. However, over the last decades, the studies performed in marine systems have been limited, recognizing the coastal environmental problem associated exclusively with the occurrence of plastic particles (synthetic polymers) (e.g., Cole et al., 2011; Hidalgo-Ruz et al., 2012). As pointed out by Athey and Erdle (2022), non-plastic anthropic particles, especially fibers, have often been excluded from studies due to the erroneous assumption that non-plastic fibers are readily biodegradable and/or ecologically harmless.

Another important question in studies of AMP is the urgency of integrating data of the anthropogenic particles (occurrence, distribution, textural characteristics, and composition), with different morphological coastal features (e.g. dunes, beaches, zones of tidal flat in bays, lagoons, or estuaries), representative of distinct sedimentary processes linked to waves (oscillatory flow), broken waves (pulsatile flow), tides, and wind action. Against this background, understanding, quantifying, and predicting the fate of AMP require the differentiation and characterization of the morphodynamics of depositional features to be analyzed based on valid diagnostic criteria, which, therefore, poses a challenge. Even recent studies that discuss AMP among coastal compartments disregard the process–form relationship in the delimitation of the sampling places (e.g., Fagiano et al., 2023; Lefebvre et al., 2023). For example, some studies have classified sediment collection sites in tidal flat sediments as "littoral zones" or "mangrove wetlands" (Naji et al., 2019; Zhou et al., 2020), while those on beaches are considered "high tide lines" or "close to shoreline" (Piñon-Colin et al., 2018; Tiwari et al., 2019). That is, coastal environments are defined in a generic way, based more on the position of variable references than on process-form relationships, resulting in a continuum of nomenclatures, which can limit the understanding of the fate of AMP. Further, detailing the different depositional features according to granulometry is crucial to understanding the occurrence of AMP, in view of the issue of hydraulic equivalence (Slingerland, 1977; Garzanti and Andò, 2007), and grain size could influence anthropogenic particle deposition and retention in sediments (Waldschläger and Schüttrumpf, 2020).

Given this overall context, this study aims to explore the occurrence, abundance, and characteristics of AMP in the coastal sediments and water of the Iguape plain in southeastern Brazil. The Iguape plain is part of the marine protected area with low population density (14.71 habitants/km^2) and occurs associated with the river basin of the Vale do Rio Ribeira declared UNESCO World Heritage site since 1999. Furthermore, it houses different natural environments, such as foredunes, tidal flats with mangroves, beaches, rivers, and areas of the Atlantic Forest. Therefore, the Iguape plain is a great opportunity to study the spatial distribution of AMP in a highly diverse coastal protected area. The main objectives of this study were to (i) quantify and characterize AMP texture (shape and size), color, and composition in sediments from well-defined coastal depositional features (tidal flats, beaches, and foredunes) and waters (sea surface and estuarine surface); (ii) characterize the granulometric distribution and respective statistics in each depositional feature and evaluate the possible relations between grain size and AMP data; and (iii) discuss the spatial distribution and accumulation of

AMP in the sedimentary substrates and surface waters of the coastal environmental protection area.

2. Materials and methods

2.1. Study area

The coastal plain of Iguape (Fig. 1A), located on the south coast of São Paulo State (Brazil), is inserted into a mosaic of conservation units, both full protection and sustainable use (MMA, 2019), with sparse and low population density (14.71 habitants/km^2). The Iguape coastal plain comprises a set of coastal morphological features, such as beaches, eolian dunes, and tidal plains, with the latter being part of a wide lagoonal-estuarine system (e.g., Bonetti Filho and Miranda, 1997). Toward the southwest, it is bordered by the estuarine channel of the Ribeira de Iguape (Fig. 1B), which represents the main continental source of terrigenous sediment to the coastline, with sedimentation rates of 5.3 mm yr^{-1} to 12.7 mm yr^{-1}, characterized by 80 % sand and 20 % muddy sediments (Tessler and Souza, 1998). The Ribeira de Iguape channel is approximately 470 km long and has a 25,000 km^2 drainage basin and an average annual water flow of 375m^3/s at its mouth (Muehe, 2012; DAEE, 2018). Water from the river is mainly used for domestic supply, reception of effluents, and agricultural purposes (Lermontov et al., 2009), with approximately 56 % of the effluents collected and 49 % treated (CETESB, 2006). It is estimated that approximately 8.8 tons of the remaining polluting load are released into the Ribeira de Iguape watershed (CETESB, 2006). The Suá Mirim River (Fig. 1B) corresponds to the channel of the Ribeira de Iguape Paleo-River (Bentz and Giannini, 2003; Prado et al., 2019), whose mouth is today blocked by foredunes located along the coastline. The margin of the Ribeira de Iguape River channel and its upper reaches are bordered by tidal flats with relatively well-preserved mangrove forests and marshes (Mahiques et al., 2013).

The seaward portion comprises Jureia beach (Fig. 1B), which is 20 km long and predominantly characterized by dissipative morphodynamics, indicating a wide foreshore (up to 240 m) with a low slope (<3°). Toward the sea, there is a formation of two or more bars parallel to the beach. In the central section of the beach, the slope (~5°) increases, and the width of the emerged part of the beach, including foreshore and discontinues backshore, decreases (90 m), which characterizes an intermediate morphodynamic. However, the northeast portion of the beach differs due to a steep slope of foreshore (<9°), a narrower emerged zone (foreshore plus continuous backshore, up to 80 m), showing reflective morphodynamic (Furlan et al., 2016). The eolian deposits along the shoreline occur in the form of active foredunes and paleodunes (Furlan et al., 2016), with dune vegetation cover of Atlantic forests (Mahiques et al., 2013).

The predominant climate in the Iguape region is the humid subtropical zone (Cfa), with hot summers (Alvares et al., 2013). The average annual temperature is above 21.2 °C, with an annual rainfall of 2268 mm that is concentrated in the summer (Schaeffer-Novelli et al., 1990). The more frequent winds come from the south and southeast (Tessler and Souza, 1998). A bimodal wave system operates, one mode from the east and northeast, and the other with waves coming from the south and southwest, related to cold weather fronts (Tessler and Souza, 1998; Alcántara-Carrió et al., 2018). Regarding wave heights, waves of 1.5 to 2 m occur in periods of 6 to 8 s (Pianca et al., 2010). The pattern of winds and waves generates bidirectional longshore drift, both in the northeast and the southwest direction (Alcántara-Carrió et al., 2018). The region is under a microtidal regime, predominantly semidiurnal, with averages of 1.2 m in the spring tide and 0.25 m in the neap tide (Mesquita and Harari, 1983).

2.2. Collection of sediment and water samples

Sample collection was carried out in August 2021 (winter), during low spring tide (0.0 to 0.1 m) under normal swell (0.5–1.0 m) and winds between 5 and 10 m/s (CPTEC/INPE data - https://www.cptec.inpe.br/). In the week preceding collection, light rainfall events occurred, around 0 mm of rain per day, reaching 12 mm/day on the day before the start of sampling. The collection method of the 62 sediment samples was adapted from Besley et al. (2017). The sampling took place in 1 m^2 plots designated at the specified sampling location. Surface sediments (5 cm thick) were collected from the four corners and the center of the sampling quadrat. At each sampling point (Fig. 1B), two 200 g samples of surface sediments were obtained, with one destined for AMP analysis and the other for grain size analysis.

Surface sediment samples were taken from the morphological features of the tidal plain, beach, and eolian dunes (Fig. 1B). In the tidal flat, the samples were collected in the infratidal margin (ITF) (n = 6), that is, the sector of the mean low tide level, and in the supratidal sector (STF) (n = 6), corresponding to the mean high tide level (Fig. 1C). In the beach system, the samples were collected at the beachface (n = 12), foreshore (n = 14) (Fig. 1D), upper foreshore, in the dissipative morphodynamic sector, or backshore in the intermediate or reflective stages. At the beachface (BF), the sampling was carried out in the submerged

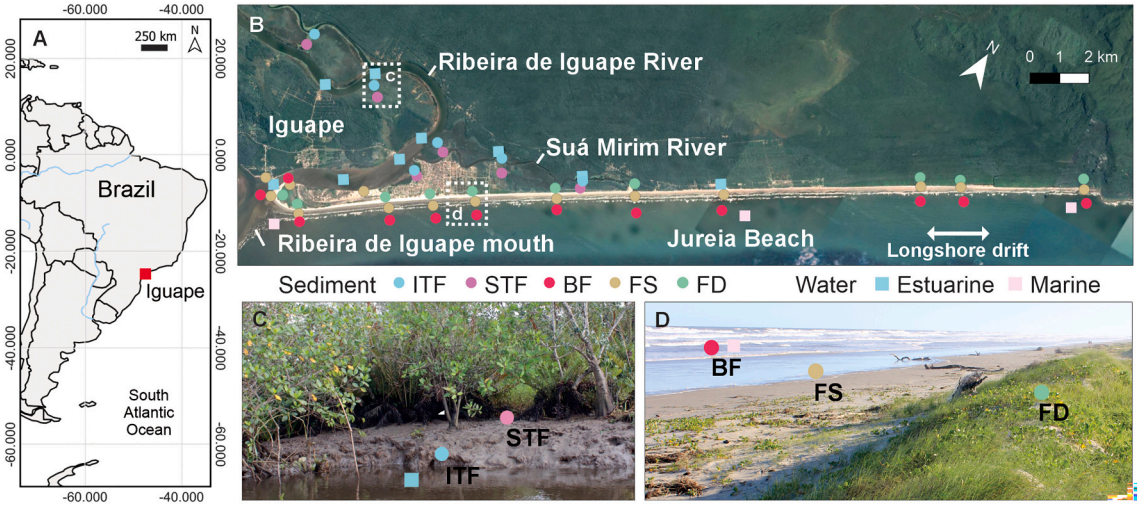

Fig. 1. Study area showing the location (A) of the sample points for AMP and grain size analysis (B) with emphasis to different morphology (C and D): infratidal flat (ITF), supratidal flat (STF), beachface (BF), foreshore (FS), and foredune (FD); and in water ("estuarine" for samples collected in estuarine channel and "marine" for beach samples). Circles and squares represent sediment and water sampling points, respectively.

zone (~1 m depth), where the water turbulence predominates over time under the action of surf waves, pulsatile flow, and longshore drift currents. At the foreshore (FS), the samples were collected in the zone that periodically emerged, which is in the upper limit of the wave that spread to the beginning of the dunes. In the foredunes (FD), 10 samples were collected at the stoss side or upwind (Fig. 1D).

Water sample collection was based on the methods described by Dubaish and Liebezeit (2013). Twelve water samples of 500 ml each were collected at a depth between 20 and 25 cm on the surface of the water column through a plastic container with a wide mouth. Six water samples were collected in the estuarine channel ("estuarine water") of the Ribeira de Iguape—three in the secondary channel of the Suá Mirim and three on the beach ("marine water") (Fig. 1B).

2.3. Quality and control of contaminants

The materials, solutions, and samples were covered with aluminum foil and opened only when necessary. All containers and instruments used were made of glass or metal. To wash the materials and prepare the saline solution, deionized water was employed, and vacuum filtered through a cellulose nitrate membrane filter (0.45 μm pore). Cotton lab coats and clothing were used to prevent clothing fibers. The workplace had limited access and controlled airflow. In laboratory proceedings, blanks were performed to qualify and quantify the background AMP contamination, undertaken simultaneously as their associated sample type. Specifically, nine blanks were executed for sediment samples, while three blanks were employed for water samples. Contamination corresponded to fibers, with a mean (± SD) of 3.76 ± 1.07 particles for the sediment samples and 2 particles for the water samples. In the blank samples for sediments, these fibers were found to be white, green, and pink, whereas in the blank samples for water, they appeared in black and white. Contamination was considered negligible, and no correction was applied to the raw data.

2.4. Extraction, identification, and classification of AMP

The separation of AMP from the 48 sediment samples was performed based on differences in density for the tidal flat samples; 5 g of dry sediment (40 °C, 96 to 144 h) was immersed in zinc chloride ($ZnCl_2$, $\rho = 1.7$ g/cm^3, Imhof et al., 2012) and manually agitated for 30 min. Next, after 12–24 h, the supernatant material was vacuum filtered through a cellulose nitrate membrane filter (0.45 μm pore) being careful not to disturb the settled sediment. The organic matter in the tidal flat samples is characterized by fragments (>0.5 cm) of plant debris (e.g., tree leaves, stems, roots, and wood), which are easily distinguishable under a stereoscope from anthropogenic microparticles. To avoid compromising the structural or chemical integrity of anthropogenic microparticles (AMP) (e.g., Hurley et al., 2018; Athey and Erdle, 2022), the samples were not subjected to removal of organic matter. Instead, for all tidal flat samples, the filter membranes (0.45 μm pore) and settled sediments were individually analyzed under a stereomicroscope.

For samples from the beach and foredunes, 10 g were manually agitated in $ZnCl_2$ for 5 min. After 10 min of stabilizing the suspension, the supernatant material was vacuum filtered (filter with 0.45 μm pore). This procedure was repeated three times. To separate AMP from water samples, vacuum filtration was used, as described by Dubaish and Liebezeit (2013). A total of 200 ml of water per sample was filtered through small pore size (0.45 μm) cellulose nitrate membrane filter with grids.

Each dried filter was observed individually under a stereomicroscope with reflected light for visual identification of all AMP extracted from all samples of the sediment and water. The classification primarily guided by criteria described in Hidalgo-Ruz et al. (2012) and Lefebvre et al. (2023). In the sedimentary samples a total of 3914 AMP were quantified, while in the water samples, 185 AMP. Briefly, to be considered AMP, particles must be of unnatural coloration and return to shape and not brittle after being pressed. The AMP were quantified and classified according to shape, color, and size. Regarding shape, AMP were classified as fibers or fragments. The AMP size was documented as the longest dimension (length) of all available AMP per sample using a stereomicroscope (Zeiss Discovery V20, 25 and 50×) with an image acquisition system (AxioVision software, image resolution 0.5 μm). AMP abundance is presented as particles/kg for dry sediment and particles/l for water.

2.5. AMP material composition

For additional characterization of AMP a fixed number of fibers (five) were extracted randomly from filter each depositional feature and water sample (Table S1). The subsampling strategy was based on fiber separation, as they were predominant in the samples (99%) and exhibited consistent visual characteristics (53-87%): uniform thickness and size, absence of cellular structure or coloration, and high tensile strength. AMP analysis was performed by Raman spectroscopy with LabRAM HR Evolution (HORIBA) equipment, using lasers of different wavelengths (473 nm, 532 nm, 633 nm, and 785 nm) and a 50× long-range objective (NA = 0.7). To obtain the spectra of the samples, parameters such as integration time, incident laser power, and accumulation were optimized. The signals were collected over a total time, typically close to 1 min. For the final measurement of the spectrum, the spectral region from 200 cm^{-1} to 3200 cm^{-1} was used. A baseline and a noise filter were applied using the software tools (LabSpec) of the micro-Raman or a Matlab® code to facilitate the identification of the material and to remove fluorescence. The compounds of the spectrum were identified using the Knowitall® database software.

From the Raman analysis and based on the criteria described by Giarratano et al. (2022), AMP were classified into: MP, modified cellulose, and dyes. MP corresponded to synthetic AMP that showed characteristic signs of polymer. Fibers of cellulose in combination with chemical additives or morphological evidence of anthropogenic alteration were considered modified cellulose. Dyes refer to fibers with the presence of a chemical additive that prevents the identification of their composition. A natural cellulose microparticle (fiber without evidence of anthropogenic modification) was identified as well as a carbon particle, possibly ash, brought by the wind. In both cases, they were not considered AMP because of a lack of confirmation of anthropogenic interference.

2.6. Grain size analysis

The grain size analysis of the 62 sediment samples was performed by laser diffraction using a Malvern Mastersizer granulometer equipped with a Hydro 2000MU module. Statistics (mean diameter and standard deviation) of the grain size distribution were calculated using the Pearson moments method from data grouped in 0.125 mm intervals.

2.7. Statistical analysis

The quantification and characterization of AMP in sedimentary samples of each morphological feature and in marine and estuarine water samples, in addition to data on the grain size of sedimentary samples, were evaluated for normalization and homogeneity using the Shapiro–Wilk test and the Levene test, respectively. All statistical analyses were done using R software (v 4.1.1, R Core Team, 2021). To assess whether there was a difference in AMP abundance and median fragment size between the morphological characteristics, the non-parametric Kruskal–Wallis test was used and post hoc pairwise Dunn's test. A one-way analysis of variance (ANOVA) was performed to identify potential differences in fiber median size and sediment grain size according to morphological features. Additionally, a two-way ANOVA was conducted to test whether the amount of AMP differed according to morphological features and sediment grain size. In the ANOVA tests (in different models), the Tukey test was performed to determine within which morphological features the differences were found. The non-

parametric Kruskal–Wallis test was used to verify whether the types of water showed statistical differences in AMP abundance and the sizes of fibers. We report statistical evidence of differences ($p < 0.05$ e.g. Peng et al., 2017; Alam et al., 2019; Falahudin et al., 2020; Marques Mendes et al., 2021; Fagiano et al., 2023), but we do not employ a strict cutoff of 0.05 (see Amrhein et al., 2019; Muff et al., 2022).

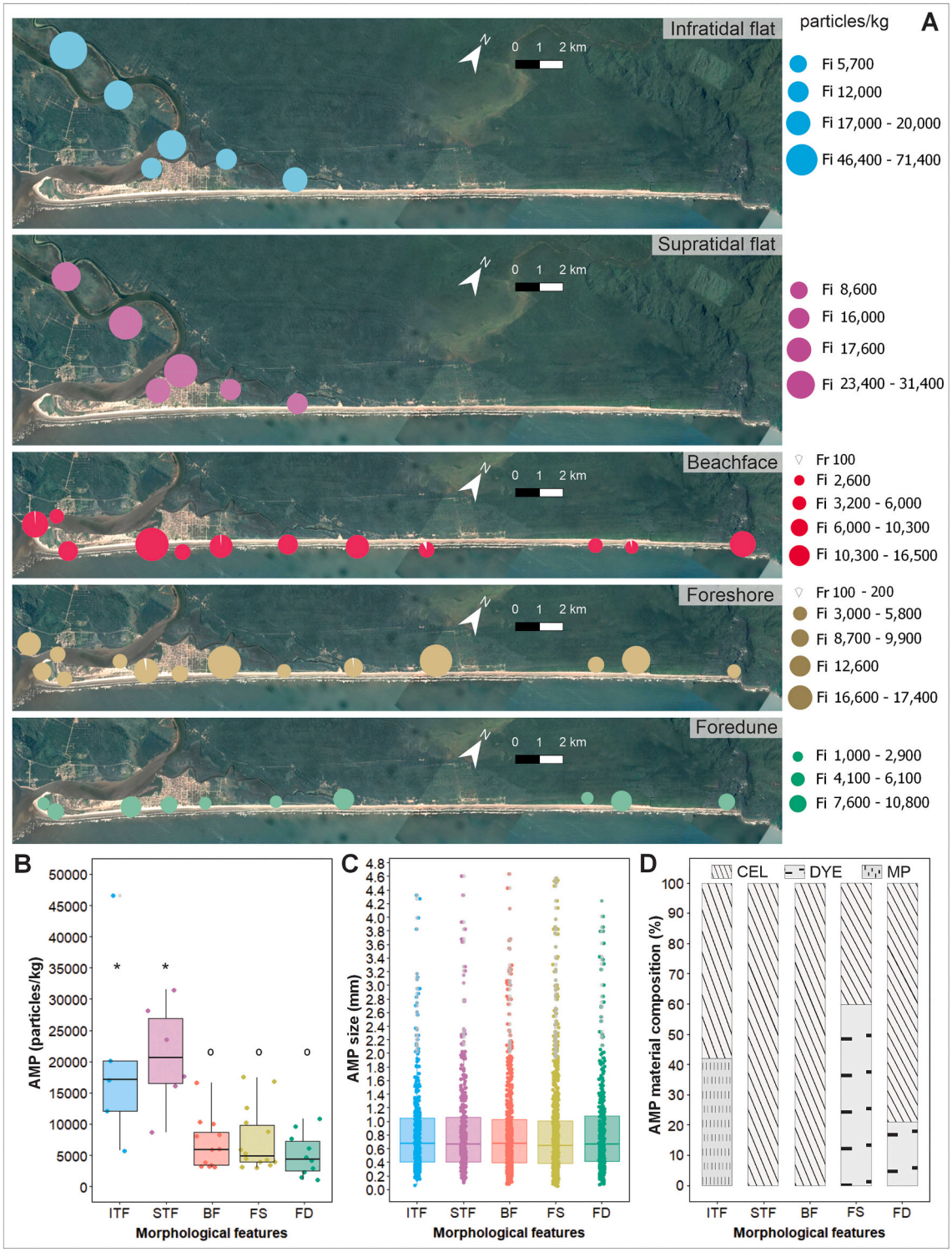

Fig. 2. AMP dataset. (A) AMP spatial distribution in sedimentary samples of infratidal flat (ITF), supratidal flat (STF), beachface (BF), foreshore (FS), and foredune (FD) for fiber (Fi) and fragment (Fr) shape. The amplitude of the circles corresponds to the abundance of AMP per sampling point. (B) Box plot for AMP abundance (particles/kg) in sedimentary samples of the same five morphological features. Features with the same symbol (° or *) do not differ from each other (Dunn's test). Differences found between FD°-ITF* ($p = 0.0007$), FD°-STF* ($p = 0.0003$), FS°-ITF* ($p = 0.0053$), FS°-STF* ($p = 0.0028$), BF°-ITF* ($p = 0.0043$) e BF°-STF* ($p = 0.0023$). (C) Box plot for AMP size variation (mm) in sediment samples of each morphological features. (D) Material composition of AMP (%) in sediment by morphological feature as for CEL (modified cellulose), DYE, and MP (microplastic).

3. Results

3.1. AMP characterization in sediments

AMP was found in all sediment samples from the Iguape plain (n = 48) and added to a total of 3914 particles. The spatial distribution of AMP in the sediments was characterized by the highest abundances in the southwest portion of the study area for samples from tidal flats (maximum 71,400 particles/kg in ITF, and 46,400 particles/kg in STF), followed by the beach samples (maximum 16,500 particles/kg in BF, and 17,400 particles/kg in FS), and foredune samples (maximum 7600 particles/kg) (Fig. 2A). The lowest AMP abundance was observed in the central portion of the beach, where the BF sediments showed maximum values of 8200 particles/kg, and the FS sediments showed maximum values of 16,600 particles/kg (Fig. 2A).

AMP abundance varied among the different morphological features (Fig. 2B). Tidal flats (ITF and STF) showed greater variability between the samples and had the highest median values, with 20,500 ± 8403 particles/kg in the STF and 18,500 ± 25,128 particles/kg in the ITF (Fig. 2B). Beach sediments (BF and FS) presented intermediate AMP abundances, with medians varying from 5900 ± 4065 particles/kg in the BF to 4700 ± 5015 particles/kg in the FS. The lowest value occurred in the eolian sediments (FD), with 4350 ± 3391 particles/kg (Fig. 2B). Differences in AMP abundance among the morphological features were evident (Kruskal–Wallis, $p = 0.0005$). AMP abundances observed in tidal flat sediments differed from abundances found in beach and foredune sediments (Dunn, $p < 0.05$) (Fig. 2B°*).

Fibers were the dominant AMP shape in all features, around 99–100 % (Figs. S1A and 2A). Fragments occurred only in beach sediments, representing 0.7 % (600 particles/kg) in the BF and 0.4 % (400 particles/kg) in the FS samples (Figs. S1B and 2A) samples. AMP exhibited a variety of colors, including black, blue, green, lavender, orange, red, colorless, white, and yellow-brown (Fig. S2A). For all samples of morphological features, the dominant colors of the fibers were colorless, with variations between 32 % and 98 %, blue between 0.37 and 35 %, and black from 0.39 to 7.75 % (Fig. S2A). The predominant color of the fragments was blue (50–67 %), followed by colorless (25–33 %) fragments (Fig. S2A). The only orange AMP was a fragment observed in the FS samples (Fig. S2A).

AMP sizes of fiber shape were similar across the morphological features, with variations from 0.1 mm to 4.6 mm and median sizes between 0.64 mm in FS and 0.68 mm in ITF (Fig. 2C). AMP fibers with a size <1 mm predominated in the morphological features. The AMP of the fragment shape had a variation size of 2.1 mm for the BF samples and 4.54 mm for the FS samples (Fig. S1B), and median sizes between 1.8 mm in FS and 2.1 mm in BF. There were no statistical differences between the morphological features for fiber size (ANOVA, $p = 1$) and fragments (Kruskal–Wallis, $p = 0.769$).

In the tidal flat sediments, the main compound found was modified cellulose, corresponding to 100 % of the microparticles in the STF and 50 % in the ITF; the remaining 50 % of the microparticles in the ITF were MP, equivalent to polypropylene (PP, 25 %) and polyethylene terephthalate (PET, 25 %) (Fig. 2D and Table S1). In beach sediments, modified cellulose corresponded to 100 % of the microparticles in the BF (a particle associated with Cromophtal Violet B), and 33 % in the FS, in which the remaining 67 % were represented by unknown material with dye (Astra blue base and Remazon Brilliant Blue BB) (Fig. 2D and Table S1). In the FD sediments, modified cellulose (80 %) was identified, 20 % was associated with Cromophtal Violet B and 20 % with Cromophtal Blue, and 20 % emitted a dye signature corresponding to Levafix Brown E-2R dye (Fig. 2D and Table S1). Typical Raman spectra are shown in Fig. S3.

3.2. Textural characteristics of sediments

In the tidal plain, muddy sediments predominated with 65 % to ITF and 80 % to STF (Fig. 3A). The beach sediments were composed of 76 % fine sand in the BF and FS, while the foredune sediments contained 73 % fine sand (Fig. 3A). The median proportion of very fine sand varied by 10 % in the BF, 11 % in the FS, and 18 % in the FD (Fig. 3A). Medium sand decreased from BF (11 %) to FD (7 %) (Fig. 3A). We found evidence of differences for medium sand concentration between the BF and STF samples (Tukey, $p = 0.05$) and for fine sand concentration between beach and FD samples and the tidal flat samples (Tukey, $p < 0.05$). In general, there was a trend toward a grain size decrease and a worsening in the sorting degree of STF and ITF sediments in relation to beach and foredunes sediments (Fig. 3B).

3.3. AMP in estuarine and marine waters

AMP were found in all 12 surface water samples, totaling 199 particles. The spatial distribution of AMP was characterized by higher abundances close to the Ribeira de Iguape mouth, both in the estuarine (maximum 280 particles/l) and marine water samples (95 particles/l) (Fig. 4A). The estuarine samples presented a median abundance of 35 ± 106.5 particles/l, with greater amplitudes of interquartile intervals between 30 and 55 particles/l (Fig. 4B). The two highest AMP abundance values in the estuarine water samples (265 and 280 particles/l) were observed close to the mouth of the river and the city of Jureia (Fig. 4A). In the seawater samples, the median was higher (85 ± 15.3 particles/l), with an interquartile range between 65 and 90 particles/l (Fig. 4B). There was no statistical difference in AMP abundance between the estuarine and marine water samples (Kruskal–Wallis, $p = 0.164$).

Fibers were predominant AMP shape in both estuarine and marine waters, representing 95 % and 80 %, respectively (Fig. 4A). Colorless fibers predominated (between 55 and 75 %), followed by black (between 20 and 25 %) (Fig. S2B), blue (between 5 and 10 %), yellow-brown (4 to 10 %), green (4 %), red (2 to 3 %), and white (2 %) fibers (Fig. S2B). The fragments were found only in gray (Fig. S2B). The fiber size ranged from 0.11 mm and the largest of 4.13 mm, with a median size of 0.65 mm, in estuarine water, and from 0.02 to 2.77 mm, with a median of 0.64 mm in marine water (Fig. 4C). No differences were observed for fiber sizes between the estuarine and marine water samples (Kruskal–Wallis, $p = 0.809$).

In the estuarine water sample, 80 % modified cellulose was identified, having a particle bound to p-acrylamide dye, and 20 % unknown material with dye referring to Cromophtal Violet K 5700 (Fig. 4D and Table S1). In marine water, the predominant compound was modified cellulose (75 %), with 50 % corresponding to modal fabric, followed by MP (25 %) from PET (Fig. 4D and Table S1).

4. Discussion

4.1. Morphodynamic processes associated with AMP transport and deposition

4.1.1. Tidal flat sediments

AMP abundance differed between tidal flat sediment samples and beach and foredune sediment samples. Tidal flat sediments exhibited the highest AMP abundance exclusively as fibers (Fig. 2A). It suggests preferential AMP accumulation on muddy sediments, which corresponds to ~80 % of the tidal flat substrate (Fig. 3A). Accordingly, the positive correlation between AMP abundance and muddy concentration reflects the reduction of sediment-carrying competence in estuarine tidal flats, where hydrodynamic flow is slower and less oscillatory (Fig. 5A) (e.g. Friedrichs, 2011). Progressive accumulation of AMP in muddy deposits also was observed in coastal sediments MP studies (e.g. Lo et al., 2018; Harris, 2020). However, the AMP abundance observed in our work (Fig. 2B) was two orders of magnitude higher than that reported by a recent review of 296 MP studies (Ouyang et al., 2022).

More specifically, our findings show a higher AMP abundance in STF compared to ITF (Fig. 2B). This result is similar MP abundance in Vitória

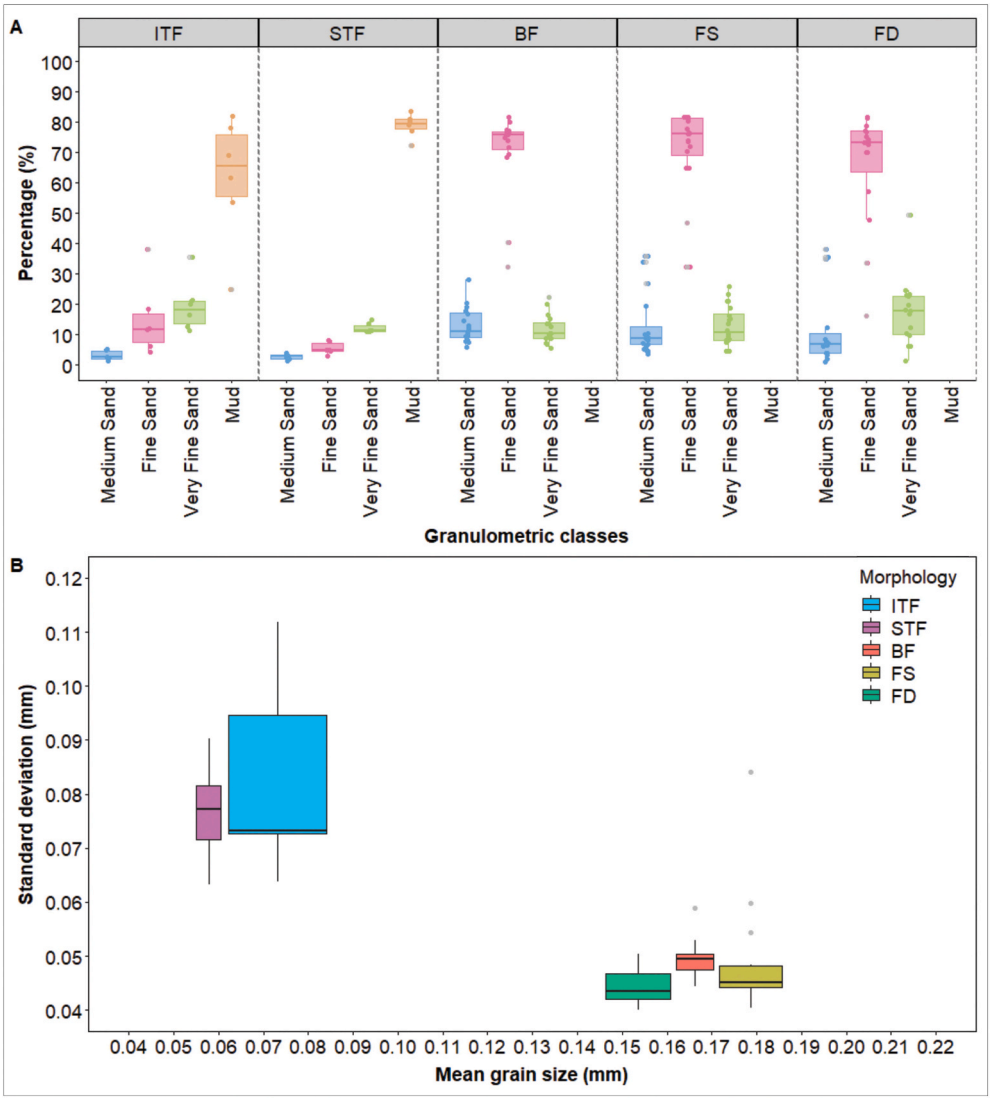

Fig. 3. Box plot for sediment grain size by morphological feature. (A) Distribution of granulometric classes. (B) Mean grain size (mm) and sorting (mm). ITF (infratidal flat), STF (supratidal flat), BF (beachface), FS (foreshore), and FD (foredune).

Bay sediments (southwest Brazil), where 66 % of the MP accumulated in upper tidal flats (Zamprogno et al., 2021). We report that a lower AMP abundance in the ITF sector may be attributed to its closer proximity to the estuarine channel margins, suggesting that fluvial or tidal flows drive AMP transportation rather than deposition (Fig. 5A).

In the case of the greater accumulation of AMP in the STF the landward buoyant particle transport gradient can have a pronounced effect. In analogy with sediment transport patterns in tidal plains (e.g. Yu et al., 2012; Shi et al., 2018) suspended AMP undergo varying advection across different water layers; this shear diffusion promotes localized resuspension and horizontal advection. This suggests that AMP has a higher potential to be transported in the landward direction, contributing to a progressive accumulation in the STF due to the decreasing energy of tidal currents. Another factor associated with the retention of AMP in tidal flats is mangrove trees' dense root system. It reduces water flow velocity (e.g. Horstman et al., 2013; Vandenbruwaene et al., 2015) and favors microparticle deposition (Fig. 5A). Therefore, mangroves may act as physical barriers to AMP dispersion, accumulating them in the vegetation and sediments of tidal flats (Sutton et al., 2016; Norris et al., 2017; Li et al., 2018a; Liu et al., 2022). It is also noted that plastic and plant debris have comparable densities (0.9–1.3 g/cm^3, see Enders et al., 2019 and Harris, 2020) and share similar float ability, favored by their predominantly elongated or platy particle shapes. So as a response to the hydraulic sorting control in the dispersion of these particles, anthropogenic microparticles and organic matter tend to be trapped in muddy sedimentary deposits (Ivar do Sul et al., 2014; Zhang et al., 2020), as water depths on the STF reduce.

Fibers AMP predominance in tidal flat sediments has also been observed elsewhere (Paes et al., 2022; Harris, 2020) and can be associated both with their availability in the immediate source area (i.e., urban centers) and with their hydrodynamic characteristics, which make them easily transported (Fig. 5B). Fibers' elongated shape and their high surface area/mass ratio keeps them buoyant in the water column (Waldschläger and Schtüttrumpf, 2019a) and make them deposit mainly under low energy and/or emerging substrate conditions (Harris, 2020), which is common in tidal flats (Fig. 5A).

Our finding revealed that AMP decreases steadily toward the estuary mouth, which may be evidence that fibers are released into the sediment from urban sources (e.g., storm drains, runoffs, and wastewater treatment plants) and from agriculture lands. Locally, wastewaters are released directly over the tidal flat area or in the channel margins of the Ribeira de Iguape River and tributaries (Lermontov et al., 2009), where only ~56 % and 49 % of the sewage are collected and treated, respectively (CETESB, 2006). Accordingly, the massive predominance of fibers

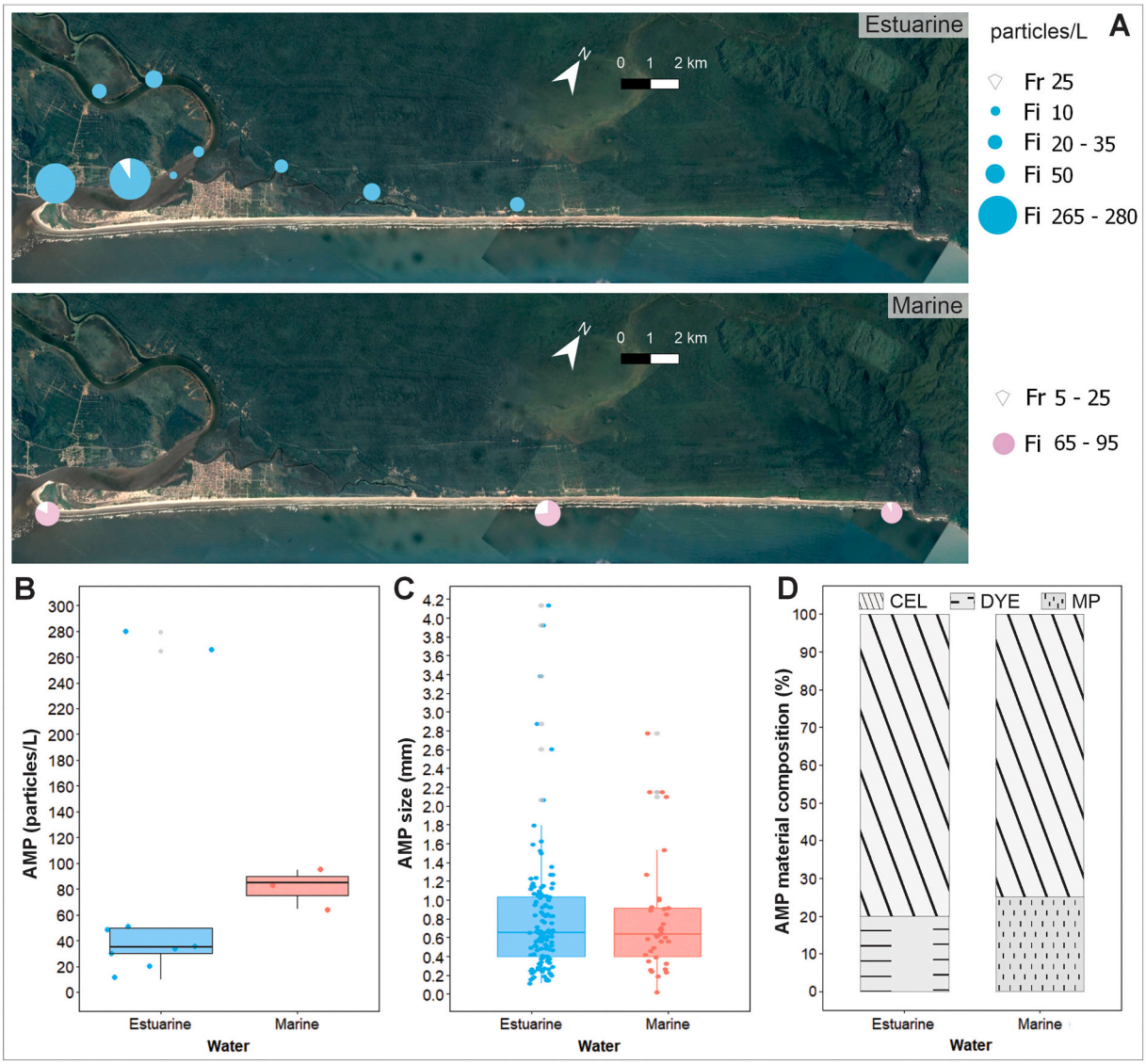

Fig. 4. AMP in estuarine and marine water samples. (A) Spatial distribution to fiber (Fi) and fragment (Fr) shape. (B) Box plot for AMP abundance (particles/l). (C) Box plot of AMP size (mm). (D) Material composition of AMP (%): CEL (modified cellulose), DYE, and MP (microplastic).

in our samples, mostly modified cellulose fibers (Fig. 2D), is likely related to textiles washing processes, an important source of AMP in coastal environments (Horton et al., 2017; Fagiano et al., 2023). Up to 700,000–1,500,000 fibers/kg can be released during a single fabric wash in a washing machine (Napper and Thompson, 2016). We do not discard that AMP in tidal flat sediments may also originate from offshore sources reaching the estuarine margin by tidal currents (Li et al., 2023).

By contrast, we only observed colorless MP fibers composed of PP and PET in ITF sediments (Table S1), whose origins may be related with single-use and short-life plastics (Avio et al., 2015; Yang et al., 2023). Alternatively, colorless PP can be originated from fishing materials (Cole et al., 2011) and PET MP may be derived from polyester fabrics (Guebitz and Cavaco-Paulo, 2008). These results suggest that, in the ITF sediments, MPA accumulation likely reflects the proximity to their source.

4.1.2. *Beach-foredune sediments*

Our results showed that AMP abundance in beach sandy (4700–5900 particles/kg) was lower than MP abundance (6870 particles/kg) in South China Sea beaches, areas with intense anthropic activities (ports and industries) (Qiu et al., 2015). Nevertheless, they were higher than that observed in Mar de la Plata (Argentina) beaches (between 184 and 1061 plastic particles/kg) (Jaubet et al., 2021). Furthermore, the prevalence of fibers is consistent with similar regional studies (e.g., Fagiano et al., 2023; Lefebvre et al., 2023) and global MP reviews (Lots et al., 2017; Harris, 2020; Curren et al., 2021). In contrast, the percentage of fragments we quantified in beach sediments (only in BF and FS with ~1 %) was substantially lower than the observed in other beaches along the Brazilian coast (99 % in Pinheiro et al., 2019; 85 % in Maynard et al., 2021; 80 % in Tsukada et al., 2021).

The beach morphodynamics may facilitate AMP spatial distributions, as previously observed for MP (e.g., Kerpen et al., 2020; Tsukada et al., 2021; Wilson et al., 2021). The predominance of dissipative morphodynamics in the study area promotes progressive AMP accumulation in beach sediments. Once the wave energy is gradually dissipated from the BS toward the FS, it generates dominant hydrodynamic conditions for mobilization, transport and deposition of sediment and AMP (Fig. 6A). In particular, the highest AMP abundance/presence in the southwest beach portion (max. 71,400 particles/kg, see Fig. 2A), may be related to longshore drift, trapping AMP in the same direction (Fig. 1C). Previous studies have shown the growth of shore-parallel elongating spits toward SW of Jureia beach and the respective blockade of littoral drift by Ribeira de Iguape River flow (Alcántara-Carrió et al., 2018),

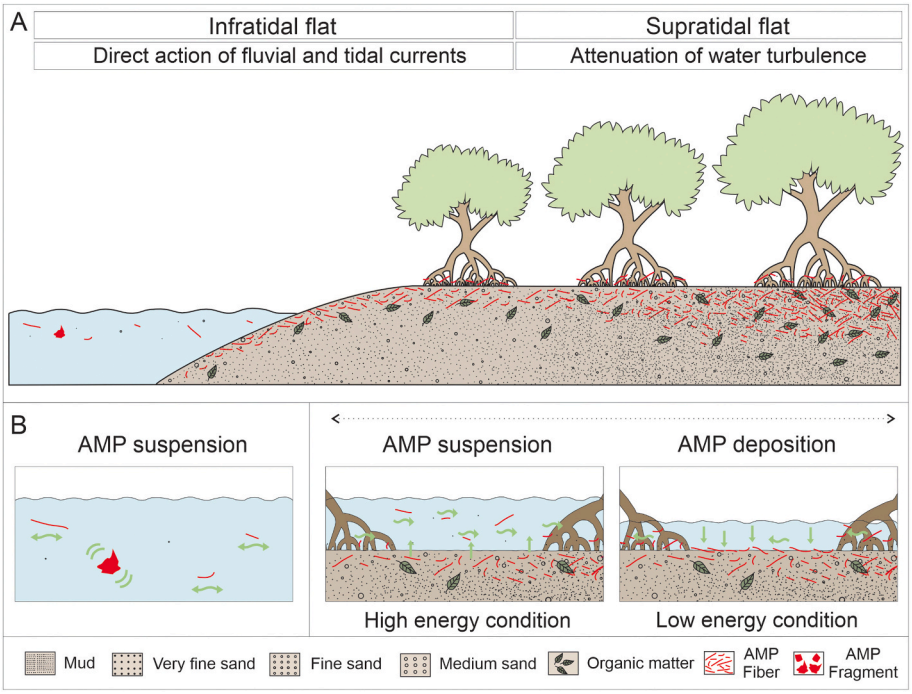

Fig. 5. Schematic transverse section of the estuarine channel margin highlighting: (A) The tidal flat morphology and respective controlling processes. (B) The form of transport and deposition of microparticles corresponding to AMP fibers, AMP fragments and organic matter in the water column and sediments.

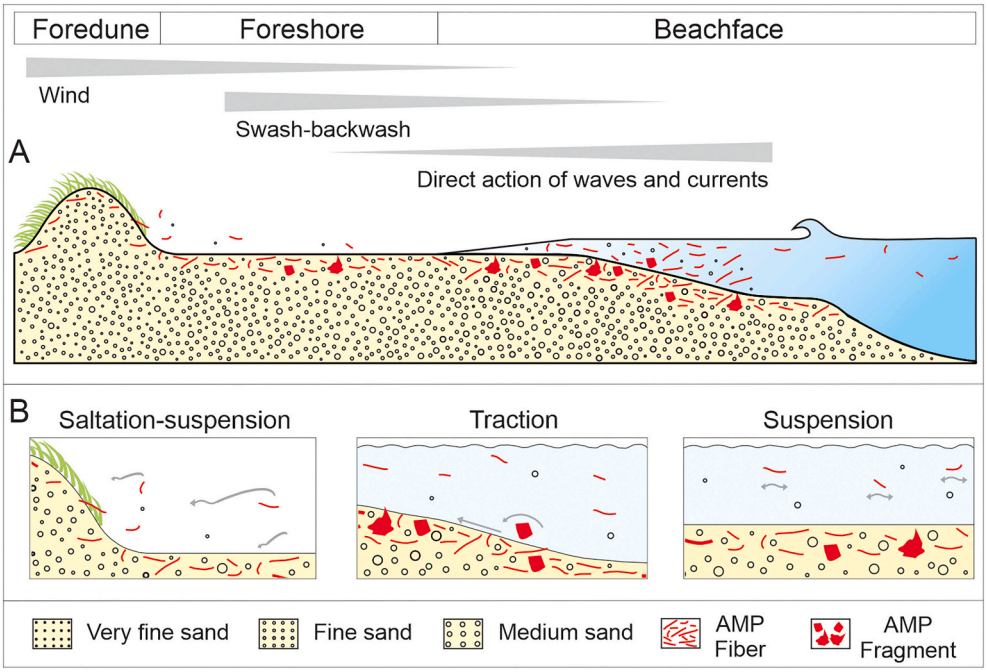

Fig. 6. Schematic transverse section of foredune, foreshore and beachface highlighting: (A) the controlling processes; (B) the form of transport and deposition of fibers and fragments in the water column and sediment.

hydrodynamic mechanisms that favor the transport and retention of AMP toward the estuary mouth.

In the beach system we observed higher medians AMP counts in BF sediments compared to FS, although no differences were detected ($p > 0.05$ see Fig. 2B). This effect of hydrodynamically homogenized particles may be a product of the local coastal processes, as the BF-FS experiences a mix of hydrodynamic forcing (waves, tides and wind), and constant bidirectional transport (swash and backwash) by breaking waves (Fig. 6A). The waves surf and breaking in the BF, tend to remobilize the sedimentary substrate near the bottom and transport AMP and sediments to the coastline, with further sorting by wave swash and backwash in the FS (Fig. 6B). Thus fibers AMP, for example, being lighter than natural sediments, tends to preferentially remain in suspension in the BF, or be re-suspended to the FS by the backwash (Fig. 6B). Consequently, in this study, the exclusive and rare (1 %) occurrence of the AMP fragments in beach sediments may reflect operation of shape and

size sorting processes by friction with the substrate in the nearby offshore source zone. Fragments AMP (MP: 1.5–2.3 g/cm^3) can be locally transported as a bedload by traction (rolling and drag) or saltation, being preferably trapped in the sands of the BF (Fig. 6B). Furthermore, the FS has greater subaerial exposure, sediment desiccation, and wind action. Therefore, lighter AMP with favorable aerodynamics, once dry, will preferably be removed from FS and taken to the foredune (Fig. 6A).

In our study, the lowest AMP abundance in the sediments was found in the FD (4350 particles/kg, Fig. 2B), with AMP exclusively in the shape of fiber. This predominance of fibers is like that observed for MP in eolian dune sediments (Costello and Ebert, 2020; Schneider and Maffessoni, 2021). AMP presence in the FD sediments is probably due to wind-driven dynamics which, like in the case of terrigenous sand grains (Gordon and McKenna Neuman, 2011), moves the particles by saltation-suspension (Fig. 6B), but at lower speeds and smaller angles. Eolian sediments showed a higher abundance of very fine sand (18 %, Fig. 3A) than beach sediment samples (~10 %, Fig. 3A), indicating selective transport by wind, favoring finer and better-sorted grains (e.g., Anderson et al., 1991). This selective transport must also act on AMP, explaining the exclusivity of fibers in FD (Fig. 2A). Because of their low density (1.4–1.5 g/cm^3), material composition (modified cellulose and dyes, Fig. 2D) and their shape, fibers are more easily transported than terrigenous sand grains and AMP of other shapes; and are more likely to remain in suspension (Waldschläger and Schüttrumpf, 2019b; Bullard et al., 2021). Thus, their deposition on the FD can be controlled by vegetation, which acts as a barrier to suspended particles transport (Fig. 6B). Additionally, fibers are easily buried and infiltrate below the surface more promptly than other AMP shapes (Costello and Ebert, 2020); or may accumulate during less vigorous wind conditions which favor deeper burial and protection from deflation events.

4.1.3. Water surface

Estuarine water samples showed AMP abundance at 35 particles/l (Fig. 4B), a value higher than that reported by Giarratano et al. (2022) for anthropogenic particles in the Chubut River (Argentina) (6.6 ± 1.4 particles/l). Marine water samples exhibited AMP abundance at 85 particles/l (Fig. 4B), which was higher than that of the estuarine water samples. This value is higher than that found for MP in marine surface waters at Claromecó beach (Argentina) (29–32 particles/l) (Truchet et al., 2021), and in Vitória (Brazil) (41.4 ± 15.7 particles/l) (Bom et al., 2022). The highest AMP abundance of AMP in the coastal water samples was observed in the mouth, mainly in the inner channel (265–280 particles/l, Fig. 4B). This pattern may be driven by tides and waves resulting in an AMP exchange between the estuarine and marine waters (Figueiredo and Vianna, 2018). In this way the estuary system both a sink and a source of AMP as already noted by Li et al. (2023). Suspended particles in the water, including AMP, tend to concentrate in the zone of maximum turbidity of the estuarine channel, located in area of convergence of river and flood tide currents. In addition, the region with the greatest AMP abundance was close to the city of Iguape and the ferries (Fig. 1C), consistent with studies showing higher MP abundance in river waters closer to urban areas (e.g., Aslam et al., 2022).

Fibers predominate in the studied waters, consistent with what has been described for microplastics in estuarine (e.g., Ibrahim et al., 2021; Rico et al., 2023) and marine waters (e.g., Barrows et al., 2018; Orona-Návar et al., 2022). Fibers in studied estuarine waters composed of modified cellulose (80 %), and unknown materials with dye (20 %) suggest origin mainly from clothing (Browne et al., 2011), which is dumped into rivers along with sewage without effective treatment (Trindade et al., 2023). Once in the rivers, the fibers are carried in suspension by the currents toward the outer estuarine waters and released into the ocean (Auta et al., 2017) along paths and during times of ebb tide dominance. This reflects the occurrence of modified cellulose in marine waters (75 %), while the blue PET fibers (25 %) possibly originated from maritime activities such as nautical sports and fishing (Browne et al., 2011). Since fibers are often lighter than water, they tend to remain floating in the water column (Waldschläger and Schüttrumpf, 2019b) under the influence of tidal and fluvial currents, waves and winds. However, PET fibers (1.39 g/ml) have a higher density than marine water (1.03 g/ml), which causes the fibers to move through the water column, going faster than other fibers, such as modified cellulose (Li et al., 2018b).

AMP fragments were found in estuarine water (5 %) and marine water (20 %) (Fig. 4A), different from the pattern observed by Castro et al. (2020) for MP in estuarine water in Niterói (Brazil), where fragments represented 54 % of the microparticles. The higher fragment abundance in marine waters than in estuarine waters suggests transport by ocean currents and fragmentation of macroplastics in beaches (Shim et al., 2018), pointing a chronic lack of solid waste management (Cheung and Fok, 2017). Fragments in the water column are transported by oscillation and rotation through the action of tidal currents and waves (Isobe et al., 2014). However, as these particles are normally denser than water, they are more likely to sink (Waldschläger and Schüttrumpf, 2019b).

Therefore, AMP transport in estuarine waters is controlled by river flow, sedimentary substrate, tidal currents, and winds (Santos et al., 2023), whereas in marine water, AMP transport is influenced by wind action, tides, waves, longshore drift currents, oceanic circulation, and sedimentary substrates (Chubarenko et al., 2018; Lefebvre et al., 2023). However, once in the water column, AMP can decompose (Weinstein et al., 2016), sink due to biofouling, which increases the microparticle density (Long et al., 2015), or be ingested by aquatic organisms later eventually deposited in deep sea and beach sediments that thus act as a significant sink for them (Chubarenko et al., 2018).

4.2. Implications of AMP size and composition for settling dynamic

In the Iguape plain, AMP sizes <1 mm were dominant in sediment samples of all morphological features and water samples. This trend corresponds to that observed in MP studies in tidal flat (Nor and Obbard, 2014), beach (Truchet et al., 2021), and eolian dune (Costello and Ebert, 2020) sediments, as well as in estuarine (Lima et al., 2014; Xu et al., 2018) and marine (Figueiredo and Vianna, 2018; Wang et al., 2021) waters. Although industrially AMP can present sizes <1 mm, the predominance of AMP <1 mm in sediments can be explained by the size decrease of larger initial particles during the residence time in natural environments, influenced by particle transport, weathering (e.g., UV irradiation, temperature, humidity) and microbiological degradation, as already confirmed for MP (Andrady, 2017). Furthermore, smaller particles exhibit greater sorption and aggregation capacity, leading to increased particle density and, consequently, favoring its deposition (Campanale et al., 2020).

Studies that have overlooked cellulosic microparticles (e.g., Lusher et al., 2014), whether natural or anthropogenic, may underestimate the abundance of AMP in natural environments. As highlighted by Athey and Erdle (2022) in their review of 308 articles on microfibers in marine, freshwater, and terrestrial ecosystems, only 38 % of the articles declared the proportion of natural and semi-synthetic fibers. Furthermore, some studies have classified modified cellulose fibers as MP (Peng et al., 2020). However, the results from this study (Figs. 2D and 4D) align with recent reports (e.g., Adams et al., 2021; Suaria et al., 2020; Genchi et al., 2023), emphasizing the importance of including non-plastic particles in studies on microparticles in water and sediment.

The material composition of AMP (Figs. 2D and 4D) reaffirms the assumption that the fibers found in this work originate mainly from the release of fibers from fabrics. During laundry, textiles release fibers varying based on their composition, age, construction, and finish (Gavigan et al., 2020). For example, cellulosic textiles shed significantly more fibers into the natural environment than synthetic textiles (Cesa et al., 2020). The lower durability of cellulosic fiber clothing and the easier release of these fibers into the environment should contribute to

the predominance of cellulosic AMP in this work. Despite cellulose having greater biodegradability than plastic (Royer et al., 2021), chemical additives in their composition influence the persistence of these particles in the natural ambient (Adams et al., 2021) and represent a greater threat to organisms. These additives can include synthetic dyes for coloring textiles (Zhu et al., 2019), which can cause harm to the ecosystem (Singh et al., 2020) and a variety of effects on organisms, such as DNA damage (da Cruz Brambilla et al., 2019), and destruction of lung tissue (Mittal et al., 2013), or even be carcinogenic or lethal (Remy et al., 2015). Furthermore, as well as MP, cellulosic AMP can accumulate and transport contaminants present in the natural environment, such as brominated and flame retardants (Saini et al., 2017).

5. Conclusion

This study analyzes and discusses the occurrence and characteristics of AMP in different coastal morpho-sedimentary features (tidal flat, beach, and foredune) and waters (estuarine and marine) in an environmental protection area. The AMP found in sediment and water samples have similar characteristics and provided the valuable finding that cellulose fibers are the predominant AMP. The greater AMP abundance in the tidal flat sediments reflects the low hydrodynamics of particle transport and deposition, making the tidal flat the main AMP sink. On the other hand, on the beach, the BF is under the direct action of breaking waves and their induced currents, and under the greater influence of wave backwash, contributing to the return of AMP to the water and helping to maintain AMP within the BF in successive cycles of AMP erosion and deposition. Meanwhile, in the FS, AMP are mainly controlled by the swash and backwash of the waves. Further, the FS is periodically submerged, which favors the drying of sediments and AMP that, due to the action of the winds, are transported to FD or back to the water. Thus, the BF and FS reciprocally act as AMP transfer zones to the sea and FD. Furthermore, the lower AMP abundance in the FD sediments appeared to be associated with the occurrence of fibers only, reflecting the selective action of eolian transport. Notably, the distribution and accumulation of AMP in sediments and waters reflect the hydro-aerodynamic forces that effectively sort AMP by size, shape, and density. More studies need to consider the transfer of AMP between different marine sedimentary environments to systematically prevent pollution.

Supplementary data to this article can be found online at https://doi.org/10.1016/j.scitotenv.2024.177479.

CRediT authorship contribution statement

Isabela Furlan: Writing – original draft, Visualization, Validation, Investigation, Formal analysis, Data curation. **Milene Fornari:** Writing – review & editing, Writing – original draft, Visualization, Validation, Supervision, Project administration, Methodology, Investigation, Formal analysis, Data curation, Conceptualization. **André Oliveira Sawakuchi:** Writing – review & editing. **Paulo César Fonseca Giannini:** Writing – review & editing, Methodology. **Jessica Dipold:** Writing – review & editing, Methodology. **Anderson Zanardi de Freitas:** Writing – review & editing. **Niklaus Ursus Wetter:** Writing – review & editing, Methodology. **Décio Semensatto:** Writing – review & editing, Supervision, Methodology.

Declaration of competing interest

The authors declare that they have no known competing financial interests or personal relationships that could have appeared to influence the work reported in this paper.

Acknowledgements

We are grateful to the Laboratório de Dinâmica Evolutiva (IB-CLP) who made samplings and this study possible. We also thank Jordana A. Zampelli for the assistance in Laboratório de Sedimentologia (IGc-USP) with laser grain-size. We would also like to thank Laboratory of Integrated Sciences (LabInSciences) for the use of the stereomicroscope and supervision with analysis of the AMP size.

This research was supported by: CAPES - Coordenação de Aperfeiçoamento de Pessoal de Nível Superior (grants 88887.700990/2022-00, Finance Code 001); FAPESP – The São Paulo Research Foundation (grants 2022/07199-6, 2021/04434-7, 2021/08565-3, 2018/19240-5, 2017/50332-0); CNPQ – The National Council for Scientific and Technological Development (grants 304866/2022-9, 304866/2022-9, 307179/2021-4, 308526/2021-0, 428341/2018-7, 314079/2021-1), and IPEN/CNEN – Nuclear and energy Research Institute (grant 2020.06.IPEN.33.PD).

Data availability

Data will be made available on request.

References

Adams, J.K., Dean, B.Y., Athey, S.N., Jantunen, L.M., Bernstein, S., Stern, G., Diamond, M.L., Finkelstein, S.A., 2021. Anthropogenic microparticles (including microfibers and microplastics) in marine sediments of the Canadian Arctic. Sci. Total Environ. 784, 147155. https://doi.org/10.1016/j.scitotenv.2021.147155.

Alam, F.C., Sembiring, E., Muntalif, B.S., Suendo, V., 2019. Microplastic distribution in surface water and sediment river around slum and industrial area (case study: Ciwalengke River, Majalaya district, Indonesia). Chemosp 224, 637–645. https://doi.org/10.1016/j.chemosphere.2019.02.188.

Alcántara-Carrió, J., Dinkel, T.M., Portz, L., Mahiques, M.M., 2018. Two new conceptual models for the formation and degradation of baymouth spits by longshore drift and fluvial discharge (Iguape, SE Brazil). Earth Surf. Process. Landf. 43. https://doi.org/10.1002/esp.4279.

Alvares, C.A., Stape, J.L., Sentelhas, P.C., Gonçalves, J.L.M., Sparovek, G., 2013. Köppen's climate classification map for Brazil. Meteorol. Z. 22 (6), 711–728. https://doi.org/10.1127/0941-2948/2013/0507.

Amrhein, V., Greenland, S., McShane, B., 2019. Retire statistical significance. Nature 567, 305–307. https://doi.org/10.1038/d41586-019-00857-9.

Anderson, R.S., Sørensen, M., Willetts, B.B., 1991. A review of recent progress in our understanding of aeolian sediment transport. In: Barndorff-Nielsen, O.E., Willetts, B. B. (Eds.), Aeolian Grain Transport 1. Springer. https://doi.org/10.1007/978-3-7091-6706-9_1.

Andrady, A.L., 2011. Microplastics in the marine environment. Mar. Pollut. Bull. 62, 1596–1605. https://doi.org/10.1016/j.marpolbul.2011.05.03.

Andrady, A.L., 2017. The plastic in microplastics: a review. Mar. Pollut. Bull. 119, 12–22. https://doi.org/10.1016/j.marpolbul.2017.01.082.

Antão-Barboza, L., Vethaak, A.D., Lavorante, B., Lundebye, A., Guilhermino, L., 2018. Marine microplastic debris: an emerging issue for food security, food safety and human health. Mar. Pollut. Bull. 133, 336–348. https://doi.org/10.1016/j.marpolbul.2018.05.047.

Aretoulaki, E., Ponis, S., Plakas, G., Agalianos, K., 2020. A systematic meta-review analysis of review papers in the marine plastic pollution literature. Mar. Pollut. Bull. 161 (A), 111690. https://doi.org/10.1016/j.marpolbul.2020.111690.

Arthur, C., Baker, J., Bamford, H., 2009. Proceedings of the international research workshop on the occurrence, effects, and fate of microplastic marine debris. National Oceanic and Atmospheric Administration technical Memorandum NOS-OR&R-30. https://marinedebris.noaa.gov/sites/default/files/publications-files/TM_NOS-ORR_30.pdf.

Aslam, M., Qadir, A., Hafeez, S., Aslam, H.M.U., Ahmad, S.R., 2022. Spatiotemporal dynamics of microplastics burden in river Ravi, Pakistan. J. Environ. Chem. Eng. 10 (3), 107652. https://doi.org/10.1016/j.jece.2022.107652.

Athey, S.N., Erdle, L.M., 2022. Are we underestimating anthropogenic microfiber pollution? A critical review of occurrence, methods, and reporting. Environ. Toxicol. Chem. 5173. https://doi.org/10.1002/etc.5173.

Auta, H.S., Emenike, C., Fauziah, S., 2017. Distribution and importance of microplastics in the marine environment: a review of the sources, fate, effects, and potential solutions. Environ. Int. 102, 165–176. https://doi.org/10.1016/j.envint.2017.02.013.

Avio, C.G., Gorbi, S., Milan, M., Benedetti, M., Fattorini, D., D'Errico, G., Pauletto, M., Bargelloni, L., Regoli, F., 2015. Pollutants bioavailability and toxicological risk from microplastics to marine mussels. Environ. Pollut. 198, 211–222. https://doi.org/10.1016/j.envpol.2014.12.021.

Barrows, A.P.W., Cathey, S.E., Petersen, C.W., 2018. Marine environment microfiber contamination: global patterns and the diversity of microparticle origins. Environ. Pollut. 237, 275–284. https://doi.org/10.1016/j.envpol.2018.02.062.

Belzagui, F., Buscio, V., Gutiérrez-Bouzán, C., Vilaseca, M., 2021. Cigarette butts as a microfiber source with a microplastic level of concern. Sci. Total Environ. 762, 144165. https://doi.org/10.1016/j.scitotenv.2020.144165.

Bentz, D., Giannini, P.C.F., 2003. Interpretação Artofotogeomorfológica da Planície Costeira de Una-Juréia. Modelo Evolutivo e Origem da Erosão na Praia da Juréia. IX Congresso da Associação Brasileira de Estudos do Quaternário, Municípios de

Peruíbe-Iguape, SP. https://repositorio.usp.br/directbitstream/6a185435-6494-4d77-8461-56299ada124d/1609829.pdf.
Besley, A., Vijver, M.G., Behrens, P., Bosker, T., 2017. A standardized method for sampling and extraction methods for quantifying microplastics in beach sand. Mar. Pollut. Bull. 114, 77–83. https://doi.org/10.1016/j.marpolbul.2016.08.055.
Bom, F.C., Brito, W.V.F., Sá, F., 2022. Microplastics concentration in bivalve of economic importance, a case study on the southeastern Brazilian coast. Reg. Stud. Mar. Sci. 52, 102346. https://doi.org/10.1016/j.rsma.2022.102346.
Bonetti Filho, J., Miranda, L.B., 1997. Estimativa da descarga de água doce no sistema estuarino-lagunar de Cananéia-Iguape. Rev. Bras. Oceanogr. 45 (1/2), 89–94. https://www.revistas.usp.br/rbo/article/view/6826/8295.
Browne, M.A., Crump, P., Niven, S.J., Teuten, E.L., Tonkin, A., Galloway, T., Thompson, R.C., 2011. Accumulation of microplastic on shorelines woldwide: sources and sinks. Environ. Sci. Technol. 45(21), 9175–9179. 10.1021/es201811s.
Bullard, J.E., Ockelford, A., O'Brien, P., Neuman, C.M., 2021. Preferential transport of microplastics by wind. Atmos. Environ. 245, 118038. https://doi.org/10.1016/j.atmosenv.2020.118038.
Campanale, C., Massarelli, C., Savino, I., Locaputo, V., Uricchio, V.F., 2020. A detailed review study on potential effects of microplastics and additives of concern on human health. Int. J. Environ. Res. Public Health 17. https://doi.org/10.3390/IJERPH17041212.
Carr, S.A., 2017. Sources and dispersive modes of micro-fibers in the environment. Integr. Environ. Assess. Manag. 13 (3), 466–469. https://doi.org/10.1002/ieam.1916.
de Carvalho, D.G., Baptista Neto, J.A., 2016. Microplastic pollution of the beaches of Guanabara Bay, Southeast Brazil. Ocean Coast. Manag. 128, 10–17. https://doi.org/10.1016/j.ocecoaman.2016.04.009.
Castro, R.O., Silva, M.L., Marques, M.R.C., Araújo, F.V., 2020. Spatio-temporal evaluation of macro, meso and microplastics in surface waters, bottom and beach sediments of two embayments in Niterói, RJ, Brazil. Mar. Pollut. Bullt. 160, 111537. https://doi.org/10.1016/j.marpolbul.2020.111537.
Cesa, F.S., Turra, A., Checon, H.H., Leonardi, B., Baruque-Ramos, J., 2020. Laundering and textile parameters influence fibers release in household washings. Environ. Pollut. 257. https://doi.org/10.1016/j.envpol.2019.113553.
CETESB, Companhia de Tecnologia de Saneamento Ambiental., 2006. Relatório de Qualidade das Águas Interiores do Estado de São Paulo, São Paulo. https://cetesb.sp.gov.br/aguas-interiores/publicacoes-e-relatorios/. Accessed June 20, 2023.
Cheung, P.K., Fok, L., 2017. Characterization of plastic microbeads in facial scrubs and their estimated emissions in mainland China. Water Res. 122, 53–61. https://doi.org/10.1016/j.watres.2017.05.053.
Chubarenko, I.P., Esiukova, E.E., Bagaev, A.V., Bagaeva, M.A., Grave, A.N., 2018. Three-dimensional distribution of anthropogenic microparticles in the body of sandy beaches. Sci. Total Environ. 628–629, 1340–1351. https://doi.org/10.1016/j.scitotenv.2018.02.167.
Cole, M., Lindeque, P., Halsband, C., Galloway, T.S., 2011. Microplasticsas contaminants in the marine environment: a review. Mar. Pollut. Bull. 62, 25882597. https://doi.org/10.1016/j.marpolbul.2011.09.025.
Costello, J.D., Ebert, J.R., 2020. Microplastic pollutants in the coastal dunes of Lake Erie and Lake Ontario, journal of Great Lakes research. J. Great Lak. Res. 46, 1754–1760. https://doi.org/10.1016/j.jglr.2020.08.001.
Critchell, K., Lambrechts, J., 2016. Modelling accumulation of marine plastics in the coastal zone; what are the dominant physical processes? Estuar. Coast. Shelf Sci. 171, 111–122. https://doi.org/10.1016/j.ecss.2016.01.036.
da Cruz Brambilla, C.M.C., Garcia, A.L.H., da Silva, F.R., Taffarel, S.R., Grivicich, I., Picada, J.N., Scotti, A., Dalberto, D., Misík, M., Knasmuller, S., da Silva, J., 2019. Amido black 10B a widely used azo dye causes DNA damage in pro-and eukaryotic indicator cells. Chemosp 217, 430–436. https://doi.org/10.1016/j.chemosphere.2018.11.026.
Curren, E., Kuwahara, V.S., Yoshida, T., Leong, S.C.Y., 2021. Marine microplastics in the ASEAN region: a review of the current state of knowledge. Environ. Pollut. 288, 117776. https://doi.org/10.1016/j.envpol.2021.117776.
DAEE, 2018. Sistema Integrado de Gerenciamento de Recursos Hídricos. Banco de Dados Hidrológicos. Dados sistematizados e consistidos pelo CTH - Centro de Tecnologia Hidráulica Financiamento Fehidro. Secretaria de Saneamento e Recursos Hídricos, São Paulo. http://www.hidrologia.daee.sp.gov.br/. (Accessed 20 June 2023).
Dehaut, A., Cassone, A., Frère, L., Hermabessiere, L., Himber, C., Rinnert, E., Rivière, G., Lambert, C., Soudant, P., Huvet, A., Duflos, G., Paul-Pont, I., 2016. Microplastics in seafood: benchmark protocol for their extraction and characterization. Environ. Pollut. 215, 223–233. https://doi.org/10.1016/j.envpol.2016.05.018.
Dubaish, F., Liebezeit, G., 2013. Suspended microplastics and black carbon particles in the jade system, southern North Sea. Water Air Soil Pollut. 224, 1352. https://doi.org/10.1007/s11270-012-1352-9.
Enders, K., Käppler, A., Biniasch, O., Feldens, P., Stollberg, N., Lange, X., Fischer, D., Eichhorn, K., Pollehne, F., Oberbeckmann, S., Labrenz, M., 2019. Tracing microplastics in aquatic environments based on sediment analogies. Sci. Rep. 9, 15207. https://doi.org/10.1038/s41598-019-50508-2.
Fagiano, V., Compa, M., Alomar, C., Rios-Fuster, B., Morató, M., Capó, X., Deudero, S., 2023. Breaking the paradigm: marine sediments hold two-fold microplastics than sea surface waters and are dominated by fibers. Sci. Total Environ. 858, 159722. https://doi.org/10.1016/j.scitotenv.2022.159722.
Falahudin, D., Cordova, M.R., Sun, X., Yogaswara, D., Wulandari, I., Hindarti, D., Arifin, Z., 2020. The first occurrence, spatial distribution and characteristics of microplastic particles in sediments from Banten Bay, Indonesia. Sci. Total Environm. 705, 135304. https://doi.org/10.1016/j.scitotenv.2019.135304.
Figueiredo, G.M., Vianna, T.M.P., 2018. Suspended microplastics in a highly polluted bay: abundance, size, and availability for mesozooplankton. Mar. Pollut. Bull. 135, 256–265. https://doi.org/10.1016/j.marpolbul.2018.07.020.
Friedrichs, C., 2011. 3.06-tidal flat morphodynamics: a synthesis. In: Wolanski, E., McLusky, D. (Eds.), treatise on estuarine and coastal science, pp. 137–170.
Furlan, I.C., Fornari, M., Buchamann, F.S.C., 2016. Variações morfológicas do sistema praia-duna frontal da Juréia, Iguape, São Paulo. XXVIII Congresso de Iniciação Científica da UNESP, In.
Garzanti, E., Andò, S., 2007. Heavy mineral concentration in modern sands: implications for provenance interpretation. In: Developments in Sedimentology. Elsevier, 58, pp. 517–545. https://doi.org/10.1016/S0070-4571(07)58020-9.
Gavigan, J., Kefela, T., Macadam-Somer, I., Suh, S., Geyer, R., 2020. Synthetic microfiber emissions to land rival those to waterbodies and are growing. PLoS One 15. https://doi.org/10.1371/journal.pone.0237839.
Genchi, L., Martin, C., Laptenok, S.P., Baalkhuyur, F., Duarte, C.M., Liberale, C., 2023. When microplastics are not plastic: chemical characterization of environmental microfibers using stimulated Raman microspectroscopy. Sci. Total Environ. 892, 164671. https://doi.org/10.1016/j.scitotenv.2023.164671.
Giarratano, E., Mauro, R.D., Silva, L.I., Tomba, J.P., Hernández-Moresino, R.D., 2022. The Chubut River estuary as a source of microplastics and other anthropogenic particles into the southwestern Atlantic Ocean. Mar. Pollut. Bull. 185, 114267. https://doi.org/10.1016/j.marpolbul.2022.114267.
Gordon, M., McKenna Neuman, C., 2011. A study of particle splash on developing ripple forms for two bed materials. Geomorp 129, 79–91. https://doi.org/10.1016/j.geomorph.2011.01.015.
Guebitz, G.M., Cavaco-Paulo, A., 2008. Enzymes go big: surface hydrolysis and functionalization of synthetic polymers. Trends Biotechnol. 26 (1), 32–38. https://doi.org/10.1016/j.tibtech.2007.10.003.
Harris, P.T., 2020. The fate of microplastic in marine sedimentary environments: a review and synthesis. Mar. Pollut. Bull. 158, 111398. https://doi.org/10.1016/j.marpolbul.2020.111398.
Hartmann, N.B., Hüffer, T., Thompson, R.C., Hassellöv, M., Verschoor, A., Daugaard, A. E., Rist, S., Karlsson, T., Brennholt, N., Cole, M., Herrling, M.P., Hess, M.C., Ivleva, N. P., Lusher, A.L., Wagner, M., 2019. Are we speaking the same language? Recommendations for a definition and categorization framework for plastic debris. Environ. Sci. Technol. 53 (3), 1039–1047. https://doi.org/10.1021/acs.est.8b05297.
Hidalgo-Ruz, V., Gutow, L., Thompson, R. C., Thiel, M., 2012. Microplastics in the marine environment: a review of the methods used for identification and quantification. Environ. Sci. Technol. 46, 3060–3075. 10.1021/es2031505.
Horstman, E.M., Dohmen-Janssen, C.M., Hulscher, S.J., 2013. Flow routing in mangrove forests: a field study in Trang province, Thailand. Cont. Shelf Res. 71, 52–67. https://doi.org/10.1016/j.csr.2013.10.002.
Horton, A.A., Walton, A., Spurgeon, D.J., Lahive, E., Svendsen, C., 2017. Microplastics in freshwater and terrestrial environments: evaluating the current understanding to identify the knowledge gaps and future research priorities. Sci. Total Environ. 586, 127–141. https://doi.org/10.1016/j.scitotenv.2017.01.190.
Huntington, A., Corcoran, P.L., Jantunen, L.M., Thaysen, C., Bernstein, S., Stern, G., Rochman, C.M., 2020. A first assessment of microplastics and other anthropogenic microparticles in Hudson Bay and the surrounding eastern Canadian Arctic waters of Nunavut. Facet 5 (1), 432–454. https://doi.org/10.1139/facets-2019-0042.
Hurley, R., Woodward, J., Rothwell, J.J., 2018. Microplastic contamination of river beds significantly reduced by catchment-wide flooding. Nat. Geosci. 11, 251–257. https://doi.org/10.1038/s41561-018-0080-1.
Ibrahim, Y.S., Hamzah, S.R., Khalik, W.M.A.W.M., Yusof, K.M.K.K., Anuar, S.T., 2021. Spatiotemporal microplastic occurrence study of Setiu wetland, South China Sea. Sci. Total Environ. 788, 147809. https://doi.org/10.1016/j.scitotenv.2021.147809.
Imhof, H.K., Schmid, J., Niessner, R., Ivleva, N.P., Laforsh, C., 2012. A novel highly efficient method for the separation and quantification of plastic particles in sediments of aquatic environments. Limnol. Oceanogr. Methods 10, 524–537. https://doi.org/10.4319/lom.2012.10.524.
Isobe, A., Kubo, K., Tamura, Y., Kako, S., Nakashima, E., Fujii, N., 2014. Selective transport microplastics and mesoplastics by drifting in coastal waters. Mar. Pollut. Bull. 89, 324–330. https://doi.org/10.1016/j.marpolbul.2014.09.041.
Ivar do Sul, J.A., Costa, M.F., Silva-Cavalcanti, J.S., Araújo, M.C.B., 2014. Plastic debris retention and exportation by a mangrove forest patch. Mar. Pollut. Bull. 78, 252–257. https://doi.org/10.1016/j.marpolbul.2013.11.011.
Jaubet, M.L., Hines, E., Elías, R., Garaffo, G.V., 2021. Factors driving the abundance and distribution of microplastics on sandy beaches in a Southwest Atlantic seaside resort. Mar. Environ. Res. 171, 105472. https://doi.org/10.1016/j.marenvres.2021.105472.
Jorquera, A., Castillo, C., Murillo, V., Araya, J., Pinochet, J., Narváez, D., Pantoja-Gutiérrez, S., Urbina, M.A., 2022. Physical and anthropogenic drivers shaping the spatial distribution of microplastics in the marine sediments of Chilean fjords. Sci. Total Environ. 814, 152506. https://doi.org/10.1016/j.scitotenv.2021.152506.
Kane, I.A., Clare, M.A., Miramontes, E., Wogelius, R., Rothwell, J.J., Garreau, P., Pohl, F., 2020. Seafloor microplastic hotspots controlled by deep-sea circulation. Science 368, 1140–1145. https://doi.org/10.1126/science.aba5899.
Kerpen, N.B., Schlurmann, T., Schendel, A., Gundlach, J., Marquard, D., Hüpgen, M., 2020. Wave-induced distribution of microplastic in the surf zone. Front. Mar. Sci. 7, 590565. https://doi.org/10.3389/fmars.2020.590565.
Kim, L., Kim, S.A., Kim, T.H., Kim, J., An, Y.J., 2021. Synthetic and natural microfibers induce gut damage in the brine shrimp Artemia franciscana. Aquat. Toxicol. 232, 105748. https://doi.org/10.1016/j.aquatox.2021.105748.
Kwak, J.I., Liu, H., Wang, D., Lee, Y.H., Lee, J., An, Y., 2022. Critical review of environmental impacts of microfibers in different environmental matrices. Comp.

Biochem. Physiol. Part - C: Toxicol. Pharmacol. 251, 109196. https://doi.org/10.1016/j.cbpc.2021.109196.
Lefebvre, C., Bihanic, F.L., Jalón-Rojas, I., Dusacre, E., Chassaigne–Viscaïno, L., Bichon, J., Clérandeau, C., Morin, B., Lecomte, S., Cachot, J., 2023. Spatial distribution of anthropogenic particles and microplastics in a meso-tidal lagoon (Arcachon Bay, France): a multi-compartment approach. Sci. Total Environ. 898, 165460. doi: https://doi.org/10.1016/j.scitotenv.2023.165460.
Lermontov, A., Yokoyama, L., Lermontov, M., Machado, M.A.S., 2009. River quality analysis using fuzzy water quality index: Ribeira do Iguape river watershed, Brazil. Ecol. Indic. 9, 1188–1197. https://doi.org/10.1016/j.ecolind.2009.02.006.
Li, J., Zhang, H., Zhang, K., Yang, R., Li, R., Li, Y., 2018a. Characterization, source, and retention of microplastic in sandy beaches and mangrove wetlands of the Qinzhou Bay, China. Mar. Pollut. Bull. 136, 401–406. https://doi.org/10.1016/j.marpolbul.2018.09.025.
Li, L., Li, M., Deng, H., Cai, L., Cai, H., Yan, B., Hu, J., Shi, H., 2018b. A straightforward method for measuring the range of apparent density of microplastics. Sci. Total Environ. 639, 367–373. https://doi.org/10.1016/j.scitotenv.2018.05.166.
Li, Y., Lu, Q., Yang, J., Xing, Y., Ling, W., Liu, K., Yang, Q., Ma, H., Pei, Z., Wu, T., Guo, H., Gao, Z., Zhao, L., Sun, J., Yang, F., Tang, X., Li, X., Zhao, D., 2023. The fate of microplastic pollution in the Changjiang River estuary: a review. J. Clean. Prod. 425, 138970. https://doi.org/10.1016/j.jclepro.2023.138970.
Liebezeit, G., Dubaish, F., 2012. Microplastics in beaches of the East Frisian Islands Spiekeroog and Kachelotplate. Bull. Environ. Contam. Toxicol. 89, 213–217. https://doi.org/10.1007/s00128-012-0642-7.
Lima, A.R.A., Costa, M.F., Barletta, M., 2014. Distribution patterns of microplastics within the plankton of a tropical estuary. Environ. Res. 132, 146–155. https://doi.org/10.1016/j.envres.2014.03.031.
Liu, X., Liu, H., Chen, L., Wang, X., 2022. Ecological interception effect of mangroves on microplastics. J. Hazard. Mater. 423, Part B, 127231. https://doi.org/10.1016/j.jhazmat.2021.127231.
Lo, H.S., Xu, X., Wong, C.Y., Cheung, S.G., 2018. Comparisons of microplastic pollution between mudflats and sandy beaches in Hong Kong. Environ. Pollut. 236, 208–217. https://doi.org/10.1016/j.envpol.2018.01.031.
Long, M., Moriceau, B., Gallinari, M., Lambert, C., Huvet, A., Raffray, J., Soudant, P., 2015. Interactions between microplastics and phytoplankton aggregates: impact on their respective fates. Mar. Chem. 175, 39–46. https://doi.org/10.1016/j.marchem.2015.04.003.
Lots, F.A.E., Behrens, P., Vijver, M.G., Horton, A.A., Bosker, T., 2017. A large-scale investigation of microplastic contamination: abundance and characteristics of microplastics in European beach sediment. Mar. Pollut. Bull. 123 (1–2), 219–226. https://doi.org/10.1016/j.marpolbul.2017.08.057.
Lusher, A.L., Burke, A., O'Connor, I., Officer, R., 2014. Microplastic pollution in the Northeast Atlantic Ocean: validated and opportunistic sampling. Mar. Pollut. Bull. 88 (1–2), 325–333. https://doi.org/10.1016/j.marpolbul.2014.08.023.
Mahiques, M.M., Figueira, R.C.L., Salaroli, A.B., Alves, D.P.V., Gonçalves, C., 2013. 150 years of anthropogenic metal input in a Biosphere Reserve: the case study of the Cananéia–Iguape coastal system, Southeastern Brazil. Environ. Earth Sci. 68, 1073–1087. https://link.springer.com/article/10.1007/s12665-012-1809-6.
Marques Mendes, A., Golden, N., Bermejo, R., Morrison, L., 2021. Distribution and abundance of microplastics in coastal sediments depends on grain size and distance from sources. Mar. Pollut. Bull. 172, 112802. https://doi.org/10.1016/j.marpolbul.2021.112802.
Maynard, I.F.N., Bortoluzzi, P.C., Nascimento, L.M., Madi, R.R., Cavalcanti, E.B., Lima, A.S., Jeraldo, V.L.S., Marques, M.N., 2021. Analysis of the occurrence of microplastics in beach sand on the Brazilian coast. Sci. Total Environ. 771, 144777. https://doi.org/10.1016/j.scitotenv.2020.144777.
Mesquita, A.R., Harari, J., 1983. Tides and tide gauges of Cananéia and Ubatuba - Brazil (lat, 24°). Internal Report Instituto Oceanográfico of the University of São Paulo 11, 1–14.
Mittal, A., Thakur, V., Gajbe, V., 2013. Adsorptive removal of toxic azo dye Amido black 10B by hen feather. Environ. Sci. Pollut. Res. 20, 260–269. https://doi.org/10.1007/s11356-012-0843-y.
MMA – Ministério da Infraestrutura e do Meio Ambiente, 2019. Plano de Manejo – APA Marinha Litoral Sul. Fundação Florestal. https://sigam.ambiente.sp.gov.br/sigam3/Default.aspx?idPagina=15389. (Accessed 20 June 2023).
Muehe, D., 2012. O litoral brasileiro e sua compartimentação. In: Geomorfologia do Brasil, Cunha SB, Guerra AJT (eds), 8th edn., 273–349.
Muff, S., Nilsen, E.B., O'Hara, R.B., Nater, C.R., 2022. Rewriting results sections in the language of evidence. Trends Ecol. Evol. 37 (3), 203–210. https://doi.org/10.1016/j.tree.2021.10.009.
Naji, A., Nuri, M., Amiri, P., Niyogi, S., 2019. Small microplastic particles (S-MPPs) in sediments of mangrove ecosystem on the northern coast of the Persian Gulf. Mar. Pollut. Bull. 146, 305–311. https://doi.org/10.1016/j.marpolbul.2019.06.033.
Napper, I.E., Thompson, R.C., 2016. Release of synthetic microplastic plastic fibres from domestic washing machines: effects of fabric type and washing conditions. Mar. Pollut. Bull. 112, 39–45. https://doi.org/10.1016/j.marpolbul.2016.09.025.
Nor, N.H.M., Obbard, J.P., 2014. Microplastics in Singapore's coastal mangrove ecosystems. Mar. Pollut. Bull. 79, 278–283. https://doi.org/10.1016/j.marpolbul.2013.11.025.
Norris, B.K., Mullarney, J.C., Bryan, K.R., Henderson, S.M., 2017. The effect of pneumato-phore density on turbulence: afield study in a Sonneratia-dominated mangrove forest, Vietnam. Cont. Shelf Res. 147, 114–127. https://doi.org/10.1016/j.csr.2017.06.002.
Orona-Návar, C., García-Morales, R., Loge, F.J., Mahlknecht, J., Aguilar-Hernández, I., Ornelas-Soto, N., 2022. Microplastics in Latin America and the Caribbean: a review on current status and perspectives. J. Environ. Manag. 309, 114698. https://doi.org/10.1016/j.jenvman.2022.114698.
Ostle, C., Thompson, R.C., Broughton, D., Gregory, L., Wootton, M., Johns, D.G., 2019. The rise in ocean plastics evidenced from a 60-year time series. Nat. Commun. 10, 1622. https://doi.org/10.1038/s41467-019-09506-1.
Ouyang, X., Duarte, C.M., Cheung, S., Tam, N.F., Cannicci, S., Martin, C., Lo, H.S., Lee, S. Y., 2022. Fate and effects of macro- and microplastics in coastal wetlands. Environ. Sci. Technol. 56 (4), 2386–2397. https://doi.org/10.1021/acs.est.1c06732.
Paes, E.S., Gloaguen, T.V., Silva, H.A.C., Duarte, T.S., Almeida, M.C., Costa, O.D.V., Bomfim, M.R., Santos, J.A.G., 2022. Widespread microplastic pollution in mangrove soils of Todos os Santos Bay, northern Brazil. Environ. Res. 210, 112952. https://doi.org/10.1016/j.envres.2022.112952.
Peng, G., Zhu, B., Yang, D., Su, L., Shi, H., Li, D., 2017. Microplastics in sediments of the Changjiang estuary, China. Environ. Pollut. 225, 283–290. https://doi.org/10.1016/j.envpol.2016.12.064.
Peng, G., Bellerby, R., Zhang, F., Sun, X., Li, D., 2020. The ocean's ultimate trashcan: Hadal trenches as major depositories for plastic pollution. Water Res. 168, 115121. https://doi.org/10.1016/j.watres.2019.115121.
Perumal, K., Muthuramalingam, S., 2022. Global sources, abundance, size, and distribution of microplastics in marine sediments - a critical review. Estuar. Coast. Shelf Sci. 264, 107702. https://doi.org/10.1016/j.ecss.2021.107702.
Pianca, C., Mazzini, P.L.F., Siegle, E., 2010. Brazilian offshore wave climate based on NWW3 reanalysis. Braz. J. Oceanogr. 58, 53–70. https://doi.org/10.1590/S1679-87592010000100006.
Pinheiro, L.M., Monteiro, R.C.P., Ivar do Sul, J.A., Costa, M.F., 2019. Do beachrocks affect microplastic deposition on the strandline of sandy beaches? Mar. Pollut. Bull. 141, 569–572. https://doi.org/10.1016/j.marpolbul.2019.03.010.
Piñon-Colin, T.D.J., Rodriguez-Jimenez, R., Pastrana-Corral, M.A., Rogel-Hernandez, E., Wakida, F.T., 2018. Microplastics on sandy beaches of the Baja California peninsula, Mexico. Mar. Pollut. Bull. 131, 63–71. https://doi.org/10.1016/j.marpolbul.2018.03.055.
Prado, H.M., Schlindwein, M.N., Murrieta, R.S.S., Nascimento Júnior, D.R.N., Souza, E. P., Cunha-Lignon, Ma., Mahiques, M.M., Giannini, P.C.F, Contente, R.F., 2019. The Valo Grande Channel in the Cananéia-Iguape estuary-lagoon complex (SP, Brazil): environmental history, ecology, and future perspectives. Ambient. Soc. (Online), 22. doi:https://doi.org/10.1590/1809-4422asoc0182r2vu19L4TD.
Qi, H., Fu, D., Wang, Z., Gao, M., Peng, L., 2020. Microplastics occurrence and spatial distribution in seawater and sediment of Haikou Bay in the northern South China Sea. Estuar. Coast. Shelf Sci. 239, Article 106757. https://doi.org/10.1016/j.ecss.2020.106757.
Qiu, Q., Peng, J., Yu, X., Chen, F., Wang, J., Dong, F., 2015. Occurrence of microplastics in the coastal marine environment: first observation on sediment of China. Mar. Pollut. Bull. 98, 274–280. https://doi.org/10.1016/j.marpolbul.2015.07.028.
R Core Team, 2021. R: A Language and Environment for Statistical Computing. R Foundation for Statistical Computing, Vienna, Austria. https://www.R-project.org/.
Remy, F., Collard, F., Gilbert, B., Compère, P., Eppe, G., Lepoint, G., 2015. When microplastic is not plastic: the ingestion of artificial cellulose fibers by macrofauna living in seagrass Macrophytodetritus. Environ. Sci. Technol. 49 (18), 11158–11166. https://doi.org/10.1021/acs.est.5b02005.
Rico, A., Redondo-Hasselerharm, P.E., Vighi, M., Waichman, A.V., Nunes, G.S.S., Oliveira, R., Singdahl-Larsen, C., Hurley, R., Nizzetto, L., Schell, T., 2023. Large-scale monitoring and risk assessment of microplastics in the Amazon River. Water Res. 232, 119707. https://doi.org/10.1016/j.watres.2023.119707.
Royer, S., Wiggin, K., Kogler, M., Deheyn, D.D., 2021. Degradation of synthetic and wood-based cellulose fabrics in the marine environment: comparative assessment of field, aquarium, and bioreactor experiments. Sci. Total Environ. 791, 148060. https://doi.org/10.1016/j.scitotenv.2021.148060.
Saini, A., Okeme, J., Parnis, J.M., McQueen, R.H., Diamond, M.L., 2017. From air to clothing: characterizing the accumulation of semi-volatile organic compounds to fabrics in indoor environments. Indoor Air 27, 631–641. https://doi.org/10.1111/ina.12328.
Santos, C.R., Drumond, G.P., Moreira, V.R., Santos, L.V.S., Amaral, M.C.S., 2023. Microplastics in surface water: occurrence, ecological implications, quantification methods and remediation technologies. Chem. Eng. J. 144936. https://doi.org/10.1016/j.cej.2023.144936.
Schaeffer-Novelli, Y., Mesquita, H.S.L., Cintrón-Molero, G., 1990. The Cananéia Lagoon Estuarine System, São Paulo, Brazil. Estuar 13, 193–203. https://doi.org/10.2307/1351589.
Schneider, I., Maffessoni, D., 2021. Quantificação de microplásticos em praias antropizadas e pouco antropizadas no litoral do Rio Grande do Sul, Brasil. Arq. Ciên. Mar. 54, 89–105. https://doi.org/10.32360/acmar.v54i1.43210.
Shi, B., Wang, Y.P., Wang, L.H., Li, P., Gao, J., Xing, F., Chen, J.D., 2018. Great differences in the critical erosion threshold between surface and subsurface sediments: a field investigation of an intertidal mudflat, Jiangsu, China. Estuar. Coast. Shelf Sci. 206, 76–86. https://doi.org/10.1016/j.ecss.2016.11.008.
Shim, W.J., Hong, S.H., Eo, S., 2018. Chapter 1 – Marine Microplastics: Abundance, Distribution, and Composition. Microplastic Contamination in Aquatic Environments. Elsevier, In, pp. 1–26. https://doi.org/10.1016/B978-0-12-813747-5.00001-1.
Singh, R.P., Mishra, S., Das, A.P., 2020. Synthetic microfibers: pollution toxicity and remediation. Chemosp 257, 127199. https://doi.org/10.1016/j.chemosphere.2020.127199.
Slingerland, R.L., 1977. The effects of entrainment on the hydraulic equivalence relationships of light and heavy minerals in sands. J. Sediment. Petrol. 47 (2), 753–770. https://doi.org/10.1306/212F7243-2B24-11D7-8648000102C1865D.

Suaria, G., Achtypi, A., Perold, V., Lee, J.R., Pierucci, A., Bornman, T.G., Aliani, S., Ryan, P.G., 2020. Microfibers in oceanic surface waters: a global characterization. Sci. Adv. 6, eaay8493. https://doi.org/10.1126/sciadv.aay8493.

Sutton, R., Mason, S.A., Stanek, S.K., Willis-Norton, E., Wren, I.F., Box, C., 2016. Microplastic contamination in the San Francisco Bay, California, USA. Mar. Pollut. Bull. 109, 230–235. https://doi.org/10.1016/j.marpolbul.2016.05.077.

Tessler, M.G., Souza, L.A.P., 1998. Dinâmica sedimentar e feições sedimentares identificadas na superfície de fundo do Sistema Cananéia-Iguape, SP. Rev. Bras. Oceanogr. 46, 69–83. https://doi.org/10.1590/S1413-77391998000100006.

Tiwari, M., Rathod, T.D., Ajmal, P.Y., Bhangare, R.C., Sahu, S.K., 2019. Distribution and characterization of microplastics in beach sand from three different Indian coastal environments. Mar. Pollut. Bull. 140, 262–273. https://doi.org/10.1016/j.marpolbul.2019.01.055.

Trindade, L.S., Gloaguen, T.V., Benevides, T.S.F., Valentim, A.C.S., Bomfim, M.R., Santos, J.A.G., 2023. Microplastics in surface waters of tropical estuaries around a densely populated Brazilian bay. Environ. Pollut. 323, 121224. https://doi.org/10.1016/j.envpol.2023.121224.

Truchet, D.M., López, A.D.F., Ardusso, M.G., Rimondino, G.N., Buzzi, N.S., Malanca, F.E., Spetter, C.V., Severini, M.D.F., 2021. Microplastics in bivalves, water and sediments from a touristic sandy beach of Argentina. Mar. Pollut. Bull. 173, 113023. https://doi.org/10.1016/j.marpolbul.2021.113023.

Tsukada, E., Fernandes, E., Vidal, C., Salla, R.F., 2021. Beach morphodynamics and its relationship with the deposition of plastic particles: a preliminary study in southeastern Brazil. Mar. Pollut. Bull. 172, 112809. https://doi.org/10.1016/j.marpolbul.2021.112809.

Vandenbruwaene, W., Schwarz, C., Bouma, T.J., Meire, P., Temmerman, S., 2015. Landscape-scale flow patterns over a vegetated tidal marsh and an unvegetated tidal flat: implications for the landform properties of the intertidal floodplain. Geomorphology 231, 40–52. https://doi.org/10.1016/j.geomorph.2014.11.020.

Waldschläger, K., Schtüttrumpf, H., 2019a. Erosion behavior of different microplastic particles in comparison to natural sediments. Environ. Sci. Technol. 53, 13219–13227. https://doi.org/10.1021/acs.est.9b05394.

Waldschläger, K., Schüttrumpf, H., 2019b. Effects of particle properties on the settling andrise velocities of microplastics in freshwater under laboratory conditions. Environ. Sci. Technol. 53. https://doi.org/10.1021/acs.est.8b06794, 1958–1066.

Waldschläger, K., Schüttrumpf, H., 2020. Infiltration behavior of microplastic particles with different densities, sizes, and shapes-from glass spheres to natural sediments. Environ. Sci. Technol. 54 (15), 9366–9373. https://doi.org/10.1021/acs.est.0c01722.

Waldschläger, K., Lechthaler, S., Stauch, G., Schüttrumpf, H., 2020. The way of microplastic through the environment – application of the source-pathway-receptor model (review). Sci. Total Environ. 713, 136584. https://doi.org/10.1016/j.scitotenv.2020.136584.

Wang, D., Su, L., Ruan, H.D., Chen, J., Lu, J., Lee, C., Jiang, S.Y., 2021. Quantitative and qualitative determination of microplastics in oyster, seawater and sediment from the coastal areas in Zhuhai, China. Mar. Pollut. Bull. 164, 112000. https://doi.org/10.1016/j.marpolbul.2021.112000.

Weinstein, J.E., Crocker, B.K., Gray, A.D., 2016. From macroplastic to microplastic: degradation of high-density polyethylene, polypropylene, and polystyrene in a saltmarsh habitat. Environ. Toxicol. Chem. 35, 1632–1640. https://doi.org/10.1002/etc.3432.

Wilson, D.R., Godley, B.J., Haggar, G.L., Santillo, D., Sheen, K.L., 2021. The influence of depositional environment on the abundance of microplastic pollution on beaches in the Bristol Channel, UK. Mar. Pollut. Bull. 164. https://doi.org/10.1016/j.marpolbul.2021.111997.

Xu, P., Peng, G., Su, L., Gao, Y., Gao, L., Li, D., 2018. Microplastic risk assessment in surface waters: a case study in the Changjiang estuary, China. Mar. Pollut. Bull. 133, 647–654. https://doi.org/10.1016/j.marpolbul.2018.06.020.

Yang, T., Zeng, Y., Kang, Z., Cai, M., Chen, K., Zhao, Q., Lin, J., Liu, R., Xu, G., 2023. Enrichment and ecological risks of microplastics in mangroves of southern Hainan Island, China. Sci. Total Environ. 889, 164160. https://doi.org/10.1016/j.scitotenv.2023.164160.

Yu, Q., Wang, Y.P., Flemming, B., Gao, S., 2012. Tide-induced suspended sediment transport: depth-averaged concentrations and horizontal residual fluxes. Cont. Shelf Res. 34, 53–63. https://doi.org/10.1016/j.csr.2011.11.015.

Zamprogno, G.C., Caniçali, F.B., Cozer, C.R., Otegui, M.B.P., Graceli, J.B., Costa, M.B., 2021. Spatial distribution of microplastics in the superficial sediment of a mangrove in Southeast Brazil: a comparison between fringe and basin. Sci. Total Environ. 784, 146963. https://doi.org/10.1016/j.scitotenv.2021.146963.

Zhang, L., Zhang, S., Guo, J., Yu, K., Wang, Y., Li, L., 2020. Dynamic distribution of microplastics in mangrove sediments in Beibu gulf, South China: implications of tidal current velocity and tidal range. J. Hazard. Mater. 399, 122849. https://doi.org/10.1016/j.jhazmat.2020.122849.

Zhou, Q., Tu, C., Fu, C., Li, Y., Zhang, H., Xiong, K., Zhao, X., Li, L., Waniek, J.J., Luo, Y., 2020. Characteristics and distribution of microplastics in the coastal mangrove sediments of China. Sci. Environ. 703, 134807. https://doi.org/10.1016/j.scitotenv.2019.134807.

Zhu, L., Bai, H., Chen, B., Sun, X., Qu, K., Xia, B., 2018. Microplastic pollution in North Yellow Sea, China: observations on occurrence, distribution and identification. Sci. Total Environ. 636, 20–29. https://doi.org/10.1016/j.scitotenv.2018.04.182.

Zhu, X., Nguyen, B., You, J.B., Karakolis, E., Sinton, D., Rochman, C., 2019. Identification of microfibers in the environment using multiple lines of evidence. Environ. Sci. Technol. 53, 11877–11887. https://doi.org/10.1021/acs.est.9b05262.